Transformation of LQR weights for Discretization Invariant Performance of PI/PID Dominant Pole Placement Controllers

Kaushik Halder[1], Saptarshi Das[2], Amitava Gupta[1]

1) Department of Power Engineering, Jadavpur University, Salt Lake Campus, LB-8, Sector 3, Kolkata-700098, India

2) Department of Mathematics, College of Engineering, Mathematics and Physical Sciences, University of Exeter, Penryn Campus, Penryn TR10 9FE, United Kingdom

Author's Emails:

kaushikhalder.pe.rs@jadavpuruniversity.in (K. Halder)

saptarshi.das@ieee.org, s.das3@exeter.ac.uk (S. Das*)

amitava.gupta@jadavpuruniversity.in (A. Gupta)

Phone number: +44-7448572598

Abstract:

Linear quadratic regulator (LQR), a popular technique for designing optimal state feedback controller is used to derive a mapping between continuous and discrete-time inverse optimal equivalence of proportional integral derivative (PID) control problem via dominant pole placement. The aim is to derive transformation of the LQR weighting matrix for fixed weighting factor, using the discrete algebraic Riccati equation (DARE) to design a discrete time optimal PID controller producing similar time response to its continuous time counterpart. Continuous time LQR-based PID controller can be transformed to discrete time by establishing a relation between the respective LQR weighting matrices that will produce similar closed loop response, independent of the chosen sampling time. Simulation examples of first/second order and first-order integrating processes exhibiting stable/unstable and marginally-stable open-loop dynamics are provided, using the transformation of LQR weights. Time responses for set-point and disturbance inputs are compared for different sampling time as fraction of the desired closed-loop time constant.

Keywords: optimal control; linear quadratic regulator (LQR); PI/PID controller tuning; dominant pole placement; discrete time control; stable-unstable-integrating test-bench

1. Introduction

PID controller is a popular choice in process control industries primarily due to its structural simplicity, robustness, good tracking, disturbance rejection etc. For effective application of PID controllers, it should be properly tuned and there are various design methodologies to determine the optimal choice of the controller parameters in order to meet the time and frequency domain design specifications [1]. In the case of complicated processes, a representative mathematical model cannot be obtained easily. Under such a scenario, design of a PID controller using analytical approach is not possible, and the tuning of PID controller is done using experimental approaches [2]. Among various other tuning methods, heuristic rule-based, gain phase margin, pole placement, D-partitioning, frequency domain shaping, interval and optimization approaches, optimal control theory, especially the LQR has been quite promising. In this method, the user-defined real symmetric positive definite matrices

($\mathbf{Q}=\mathbf{Q}^T \geq 0, \mathbf{R}=\mathbf{R}^T > 0$), also known as the weighting matrix and weighting factor respectively, play a major role [3]. These matrices correspond to the state variables (x) and the control action (u) with an associated minimizing control cost (J). These weighting matrices balance the penalties on the excursion of state variables and control effort. These LQR weights are used to solve the continuous algebraic Riccati equation (CARE) as well as the discrete algebraic Riccati equation (DARE) for the continuous and discrete time cases respectively, to find out a matrix solution ($\mathbf{P}$) which is also real symmetric positive definite [4]. An optimal state feedback gain can be achieved by this matrix solution of Riccati equation in continuous or discrete time and finally to derive the optimal control law. These optimal state feedback gains in continuous-time ($\mathbf{K_s}$) or discrete-time ($\mathbf{K_s}$) are therefore used as the PID controller gains. It is understandable that such an optimally designed continuous time LQR based PID controller, meeting certain time domain specifications thus may not perform well under arbitrary discretization schemes or sampling time (T_s). Theoretical results regarding sampling time sensitivity on the optimal regulators for discretization and the associated loss of controllability has been shown in [5]. Under such a scenario, directly a discrete time LQR formulation should be used instead, for designing the digital PID controller. But the problem of mapping the time domain performance specifications (or the desired dominant pole locations) onto the LQR weighting matrices has not been addressed in the literature before. Therefore, here we propose a technique that first designs a continuous time LQR-based PID controller using some user-demanded time domain specifications to calculate the LQR weights, as an integrated approach within the dominant pole placement method. Then for digital implementation of PI/PID controllers, the control system (combining the process under control and the integro-differential operators of the PID controller except the gains) is discretized and the state feedback gains are determined using a transformation of the continuous time LQR weighting matrices to obtain the optimal discrete time PID controller, even though the sampling time is chosen arbitrarily.

The pole placement and dominant pole placement methods have already been popular for PID controller design [1] which are commonly used to specify the desired closed loop control system performance. The pole placement tuning method cannot be applied directly for significantly long-time delay, because in the presence of long delay, the characteristic equation becomes infinite-dimensional. The user specified choice of performance indicators like closed loop damping (ζ_{cl}) and natural frequency (ω_{cl}) are used in guaranteed dominant pole placement [6]. This methodology assumes that the closed loop system behaves like a typical second order system and rest of the closed loop poles should lie far away from the imaginary axis and has negligibly small effect on the overall closed loop process dynamics [6]. It requires the dominance of the specified complex conjugate closed loop poles over the real undesired pole so that the closed loop system behaves almost like a second order system with specified damping and natural frequency. In other words, the real non-dominant pole must have a larger negative magnitude than the magnitude of the real part of complex conjugate dominant poles [6].

Significant amount of work has been done on merging the two concepts of PID controller design i.e. dominant pole placement [6]–[11] and inverse optimal LQ control [12]–[17]. Fujinaka and Katayama [18] proposed the design of a discrete optimal controller with pole-placement constraints. He *et al.* [19] have introduced a method of tuning PID controllers using LQR approach for lower order systems with time delay. However, such a design is based on continuous time approach, followed by discretization with a fixed sampling time which does not guarantee that the specified time response characteristics will be met by the corresponding discrete time version of the controller as well which forms the main motivation for the investigations reported here.

The objective of this paper is to design the $\mathbf{Q}$ matrix of the discrete time LQR for which the system's response will closely match with that obtained through the original continuous time optimal controller, before discretization. In the present design context, the weighting factor $\mathbf{R}$ is chosen as unity as in [20]

and then the mapping between discrete and continuous time weighting matrices ($\mathbf{Q}$ and $\mathbf{Q}$) is attempted. In order to achieve a close enough time domain performance for the system using continuous and discrete time optimal PI/PID controllers, the weighting matrix $\mathbf{Q}$ should be designed in such a way that the desired closed loop poles and the performance of the closed loop system remains almost unchanged, while considering weighting factor $\mathbf{R}$ to be fixed in both the continuous and discrete time versions. The matrix $\mathbf{Q}$ is first analytically derived for the continuous time design and then transformed in discrete time such that the controller yields similar closed loop performance as with the continuous time controller. The parameters of the discrete time controller are then determined by solving the DARE with the transformed $\mathbf{Q}$ matrix. The corresponding discrete time PID controller produces the specified time response, similar to that with the continuous time controller. Here we extend the method proposed in [19] from classical pole placement to dominant pole placement PID controller design for three different system structures (first/second order and first order integrating) which automatically guarantees LQR optimality in both continuous and discrete time. Optimum LQR weight selection has also been discussed in continuous time [21] and discrete time [22] for designing optimal PID controllers. Within the LQR framework, the multi-objective optimum weight selection in the presence of large process delay has been addressed in [23] using two different transformations of the continuous time Riccati equation. The optimum weight selection has also been extended for the noisy tracking (integral) problem using linear quadratic Gaussian (LQG) control with loop transfer recovery (LTR) for improved stability margins [24]. Also, optimal state-feedback PD controller design has been previously studied with minimum norm controller gain to reduce noise amplification in [25], [26], [27]. But previous literatures shown above, do not provide the transformation to directly map time domain specifications (usually adopted in dominant pole placement design) onto the discrete time LQR weights, which is the main contribution of this paper over existing literatures.

Rest of the paper is organized as follows: section 2 reports guaranteed dominant pole placement through PID controlled second order system and derives the analytical expressions for the continuous and discrete time LQR weighting matrix, followed by establishing the transformation between them. Section 3 extends the method for first order integrating system with PID controllers while the same method is extended for PI controlled first order system in section 4. Simulation results on test-bench systems are reported in section 5 with time domain tracking, disturbance rejection, control effort and root-locus analysis. Discussions on the achievements and limitations of the proposed controller design approach are put forward in section 6. The paper ends in section 7, followed by the references.

2. Continuous and discrete time PID controller tuning using dominant pole placement for second order system with continuous/discrete time LQR

2.1. Dominant pole placement tuning of PID controllers for second order systems

Let us consider a second order system (1) with oscillatory/sluggish open loop dynamics:

$$G_1(s) = K \Big/ \left(\tau^2 s^2 + 2\zeta_{ol} \tau s + 1 \right), \tag{1}$$

that has to be controlled by a PID controller of the structure (2) where $\{K, \tau, \zeta_{ol}\}$ are the open loop DC gain, time constant and damping ratio and $\{K_p, K_i, K_d\}$ are the proportional and integro-differential gains of the PID controller:

$$C_1(s) = K_p + \frac{K_i}{s} + K_d s. \tag{2}$$

Then the closed loop transfer function becomes (3):

$$G_{1cl}(s) = C_1 G_1 / (1 + C_1 G_1)$$
$$= \frac{K(K_d s^2 + K_p s + K_i)}{\tau^2 s^3 + s^2(2\zeta_{ol}\tau + KK_d) + s(1 + KK_p) + KK_i}. \quad (3)$$

It is clear that the closed loop system (3) has three poles and two zeroes which changes their position based on the controller gains. Let us assume that the PID gains are selected in such a manner that the characteristic equation (3) has one real pole and two complex conjugate poles with fixed damping and frequency that corresponds to the specified closed loop system response. Then neglecting the dynamics of the closed loop zeros in (3), the desired characteristic equation $\Delta(s)$ can be represented as (4) [20]:

$$\Delta(s) = (s + m\zeta_{cl}\omega_{cl})(s^2 + 2\zeta_{cl}\omega_{cl}s + \omega_{cl}^2) = 0, \quad (4)$$

where, *m* is a positive parameter which is chosen to suitably place the closed loop real pole with respect to the complex conjugate poles. Here, ζ_{cl} is the desired closed loop system's damping ratio and ω_{cl} is the desired natural frequency of the closed loop system.

It is also clear that the closed loop system (4) has one real pole at $(s_1 = -m\zeta_{cl}\omega_{cl})$ and two complex conjugate poles at $\left(s_2, s_3 = -\zeta_{cl}\omega_{cl} \pm j\omega_{cl}\sqrt{1-\zeta_{cl}^2}\right)$. For guaranteed dominant pole placement of the closed loop system (3), the real pole has to be far away from the imaginary axis as compared to the real part of the complex conjugate poles, following the criterion in (5):

$$\zeta_{cl}\omega_{cl} \le m\zeta_{cl}\omega_{cl} \quad \Rightarrow 1 \le m. \quad (5)$$

It is also obvious that the real and complex poles of the corresponding discrete time system will be at $\left(z_1 = \exp(s_1 T_s) = \exp(-m\zeta_{cl}\omega_{cl}T_s)\right)$ and $\left(z_2, z_3 = \exp\left(-\zeta_{cl}\omega_{cl} \pm j\omega_{cl}\sqrt{1-\zeta_{cl}^2}\right)T_s\right)$, where T_s refers to the sampling time used for discretization. In order to ensure that the discrete time system is stable, these poles must be bounded within the unit circle $|z| < 1$.

In most real-world applications, the PID controller is implemented in discrete time in the form of a computer algorithm and the real process being controlled is normally in continuous time. The closed loop system's response is then sampled in regular intervals at predefined time instants by the sensor. Therefore, the closed loop system is also a discrete time system. However, even if the dominant pole placement parameter *m* is chosen properly in continuous time for arbitrary sampling time, the discretized controller designed using the continuous time LQR cannot guarantee a close enough response to the original continuous time system.

2.2. Optimal state feedback design for PID controllers via continuous time LQR

For continuous time PID controller design, the LQR approach can be used as proposed in [19] where the structure of the controller along with second order process can be represented in Figure 1(a). The system $G_1(s)$ in Figure 1(a) represents a stable time invariant second order system, characterized by its natural frequency $\omega_{ol} = 1/\tau$, damping ratio ζ_{ol} and DC gain *K*. To formulate an LQR controller, the external set point $r(t)$ is assumed to be zero as it does not affect the state feedback regulator design [19]. Therefore, error and output are related as $e = r - y = -y$. So, the above closed loop system yields the state space model as (6):

$$\dot{x}_1 = x_2, \dot{x}_2 = x_3, \dot{x}_3 = -\left(\frac{1}{\tau^2}\right)x_2 - \left(\frac{2\zeta_{ol}}{\tau}\right)x_3 - \left(\frac{K}{\tau^2}\right)u, \tag{6}$$

where, $x_1 = \int_0^t e(\tau)d\tau, x_2 = e(t) = \dot{x}_1, x_3 = \frac{de(t)}{dt} = \dot{x}_2 = \ddot{x}_1.$

The derivative of the error signal x_3 and integral of the error are introduced as the state variable x_1. Using (6), the augmented state-space model may be represented in the form (7) and the system matrices are given in (8) as:

$$\dot{\mathbf{x}}(t) = \mathbf{A}\mathbf{x}(t) + \mathbf{B}u(t), y(t) = \mathbf{C}\mathbf{x}(t), \tag{7}$$

where, $\mathbf{x}(t) = \begin{bmatrix} x_1(t) & x_2(t) & x_3(t) \end{bmatrix}^T$ and

$$\mathbf{A} = \begin{bmatrix} 0 & 1 & 0 \\ 0 & 0 & 1 \\ 0 & -\frac{1}{\tau^2} & -\frac{2\zeta_{ol}}{\tau} \end{bmatrix}, \mathbf{B} = \begin{bmatrix} 0 \\ 0 \\ -\frac{K}{\tau^2} \end{bmatrix}, \mathbf{C} = \begin{bmatrix} 0 & 1 & 0 \end{bmatrix}. \tag{8}$$

Now to design the controller, the cost function is assumed in the standard quadratic form [28] as:

$$J_c = \frac{1}{2}\int_0^\infty \left[\mathbf{x}^T(t)\mathbf{Q}\mathbf{x}(t) + u^T(t)\mathbf{R}u(t)\right]dt. \tag{9}$$

To obtain an optimal controller, the cost function (9) is minimized which gives the control law in terms of the state variables as in (10):

$$u(t) = -\mathbf{K}_s\mathbf{x}(t) = -\mathbf{R}^{-1}\mathbf{B}^T\mathbf{P}\mathbf{x}(t), \tag{10}$$

where, $\mathbf{P}$ is a symmetric positive definite matrix and the solution of the CARE is given in (11) as:

$$\mathbf{A}^T\mathbf{P} + \mathbf{P}\mathbf{A} - \mathbf{P}\mathbf{B}\mathbf{R}^{-1}\mathbf{B}^T\mathbf{P} + \mathbf{Q} = \mathbf{0}. \tag{11}$$

It is well known to design regulators in optimal control by keeping $\mathbf{R}$ fixed, while varying $\mathbf{Q}$ [12], [20].

For the third order system (8), the general form of $\{\mathbf{P}, \mathbf{Q}, \mathbf{R}\}$ matrices are in the form of (12):

$$\mathbf{P} = \begin{bmatrix} P_{11} & P_{12} & P_{13} \\ P_{21} & P_{22} & P_{23} \\ P_{31} & P_{32} & P_{33} \end{bmatrix}, \mathbf{Q} = \begin{bmatrix} Q_{11} & Q_{12} & Q_{13} \\ Q_{21} & Q_{22} & Q_{23} \\ Q_{31} & Q_{32} & Q_{33} \end{bmatrix}, \mathbf{R} = R. \tag{12}$$

It is also a common practice to choose $\mathbf{Q}$ as a diagonal matrix while setting $\mathbf{R}$ as unity (13), as also shown in [19], i.e.

$$\mathbf{Q}=\begin{bmatrix} Q_{11} & 0 & 0 \\ 0 & Q_{22} & 0 \\ 0 & 0 & Q_{33} \end{bmatrix}, \mathbf{R}=1. \tag{13}$$

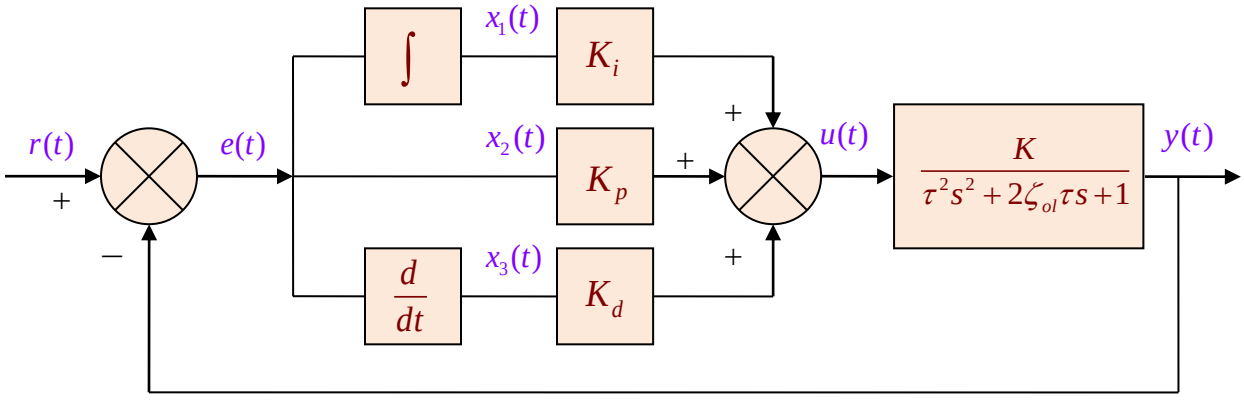

(a)

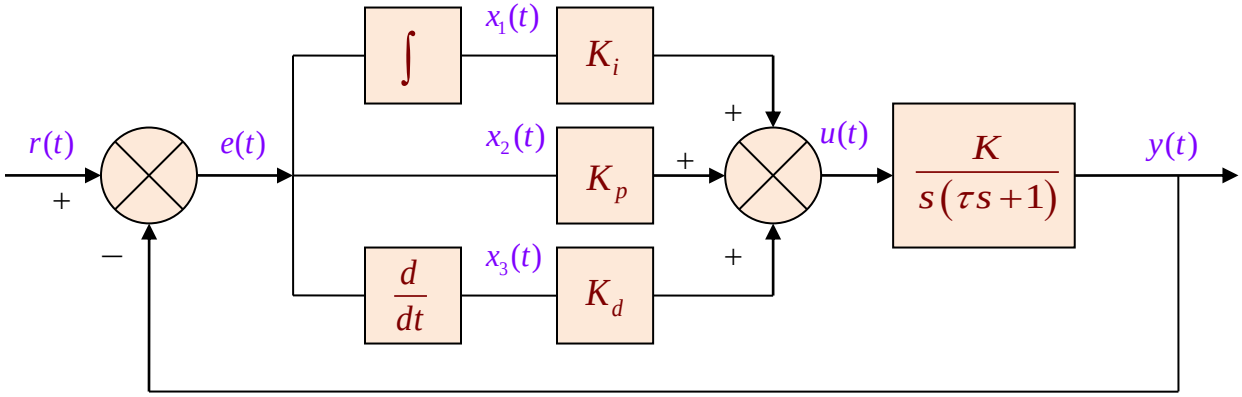

(b)

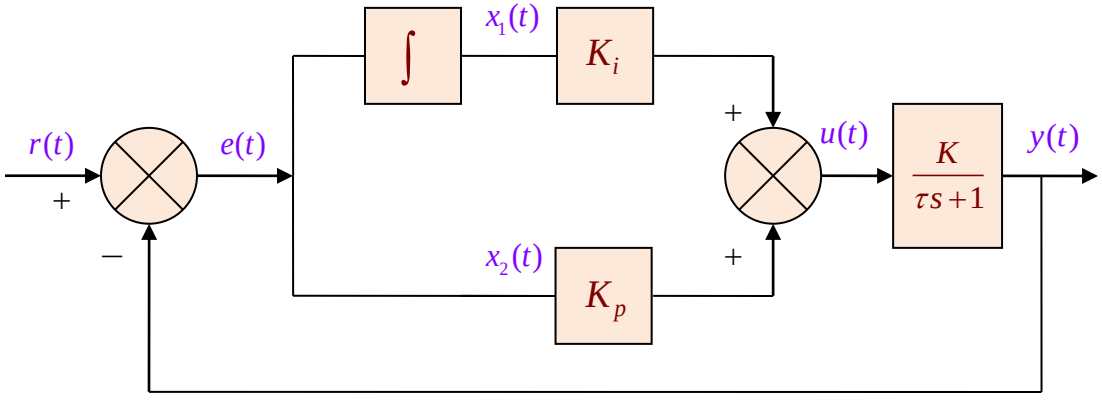

(c)

Figure 1: State variable formulation of the control system (a) PID controlled second order system, (b) PID controlled first order integrating system, (c) PI controlled first order system.

Then using (8), (10) and (12) the state feedback gain matrix ($\mathbf{K_s}$) becomes (14), i.e.

$$\mathbf{K_s} = \mathbf{R^{-1}}\begin{bmatrix} 0 & 0 & -\frac{K}{\tau^2} \end{bmatrix}\begin{bmatrix} P_{11} & P_{12} & P_{13} \\ P_{12} & P_{22} & P_{23} \\ P_{13} & P_{23} & P_{33} \end{bmatrix} = \mathbf{R^{-1}}\begin{bmatrix} -\frac{KP_{13}}{\tau^2} & -\frac{KP_{23}}{\tau^2} & -\frac{KP_{33}}{\tau^2} \end{bmatrix} = -\begin{bmatrix} K_i & K_p & K_d \end{bmatrix}, \quad (14)$$

where, $\{K_i, K_p, K_d\}$ are the integral, proportional, derivative gains of a PID controller respectively.

Then the elements $\{P_{13}, P_{23}, P_{33}\}$ of $\mathbf{P}$ matrix in (12) can be derived using (14) in the form of PID controller gain as:

$$\left.\begin{aligned} P_{13} &= R\tau^2 K_i / K \\ P_{23} &= R\tau^2 K_p / K \\ P_{33} &= R\tau^2 K_d / K \end{aligned}\right\}. \quad (15)$$

Now, the closed loop system matrix $\mathbf{A_c}$ is given by (16):

$$\mathbf{A_c} = \mathbf{A} - \mathbf{BK_s} = \begin{bmatrix} 0 & 1 & 0 \\ 0 & 0 & 1 \\ -\frac{KK_i}{\tau^2} & -\frac{(1+KK_p)}{\tau^2} & -\frac{(2\zeta_{ol}\tau + KK_d)}{\tau^2} \end{bmatrix}. \quad (16)$$

The corresponding characteristic equation of the closed loop system represented in equation (3) is given by (17):

$$\Delta_1(s) = s^3 + \left(\frac{2\zeta_{ol}\tau + KK_d}{\tau^2}\right)s^2 + \left(\frac{1+KK_p}{\tau^2}\right)s + \frac{KK_i}{\tau^2} = 0. \quad (17)$$

The desired closed loop characteristic equation $\Delta_2(s)$ from (4) can be rewritten as (18):

$$\Delta_2(s) = s^3 + (2+m)\zeta_{cl}\omega_{cl}s^2 + (1+2m\zeta_{cl}^2)\omega_{cl}^2 s + m\zeta_{cl}\omega_{cl}^3 = 0. \quad (18)$$

Comparing the coefficients of the actual characteristic equation $\Delta_1(s)$ in (17) with the desired system characteristic equation $\Delta_2(s)$ in (18), the PID controller gain are obtained in (19) as:

$$\left.\begin{aligned} K_i &= m\zeta_{cl}\omega_{cl}^3\tau^2/K \\ K_p &= \left(\left(1+2m\zeta_{cl}^2\right)\tau^2\omega_{cl}^2-1\right)/K \\ K_d &= \left(\left(2+m\right)\tau^2\zeta_{cl}\omega_{cl}-2\zeta_{ol}\tau\right)/K \end{aligned}\right\}. \tag{19}$$

The symmetric property $\mathbf{P}=\mathbf{P}^T$ is used here to derive the other elements of $\mathbf{P}$ matrix and diagonal elements of weighting matrix $\mathbf{Q}$ while rest of the elements of $\mathbf{Q}$ matrix are assumed to be zero. Also, th rest of the elements of $\mathbf{P}$ matrix and the diagonal elements of $\mathbf{Q}$ matrix i.e.$\{Q_{11},Q_{22},Q_{33}\}$ can be obtained as (20) and (21) using equation(8), (11)-(15) and (19), i.e.

$$\left.\begin{aligned} P_{11} &= \left(P_{13}+R^{-1}K^2P_{13}P_{23}\right)/\tau^2 \\ P_{12} &= \left(2\zeta_{ol}\tau P_{13}+R^{-1}K^2P_{13}P_{33}\right)/\tau^2 \\ P_{22} &= \left(2\zeta_{ol}\tau P_{23}+R^{-1}K^2P_{23}P_{33}+P_{33}-\tau^2P_{13}\right)/\tau^2 \end{aligned}\right\}, \tag{20}$$

$$\left.\begin{aligned} Q_{11} &= RK_i^2 = R^{-1}K^2P_{13}^2/\tau^2 \\ Q_{22} &= -\frac{2P_{12}K-2RK_p-RK_p^2K}{K} = \left(R^{-1}K^2P_{23}^2-2\left(\tau^2P_{12}-P_{23}\right)\right)/\tau^2 \\ Q_{33} &= \frac{R\left(-2K_p\tau^2+4K_d\tau\zeta_{ol}+KK_d^2\right)}{K} = \left(R^{-1}K^2P_{33}^2-2\left(\tau^2P_{23}-2\zeta_{ol}\tau P_{33}\right)\right)/\tau^2 \end{aligned}\right\}. \tag{21}$$

Therefore, the continuous time LQR weight $\mathbf{Q}$ can be achieved in terms of the pole placement parameter *m*, specified by the desired closed loop performance $\{\zeta_{cl},\omega_{cl}\}$ and the open loop system characteristics $\{K,\zeta_{ol},\omega_{ol}\}$. The advantage of the LQR based PID controller is using minimum controller effort to ensure minimum deviation of the state trajectories.

2.3. Digital PID controller design via discrete time LQR and novel transformation of the LQR weights

The continuous time optimal PID controller thus obtained can now be discretized by appropriate choice of the sampling time (T_s). However, introduction of the sampler and the zero order hold (ZOH) does not guarantee the fact that the controller thus obtained will also be optimal or shall meet the desired characteristics specified in the continuous time domain [28]. This problem can be addressed by finding out a transformation of the discrete LQR weight ($\mathbf{Q}$) in terms of specified parameters in continuous time such that there is minimal difference between the obtain controller gains between the continuous and discrete time [29]. This will ensure that the specifications of the continuous time optimal controller are met in the discrete time implementation as well, with arbitrary selection of sampling time for discretization. The issue of optimality is addressed by transforming the $\mathbf{Q}$ matrix in (21) appropriately, so that when the transformed $\mathbf{Q}$ matrix is used in the DARE, the solution can be used to design a PID controller that guarantees optimality in discrete time. This should also ensure maintaining the specified time response as obtained with the continuous time controller.

The discretized system matrices can be obtained using the specified sampling time T_s and identity matrix ($\mathbf{I}$) as in (22):

$$\mathbf{G} = e^{\mathbf{A}T_s} = \mathbf{I} + \mathbf{A}T_s$$
$$\mathbf{H} = \int_0^{T_s} e^{\mathbf{A}\lambda}\mathbf{B}d\lambda = \mathbf{A}^{-1}\left(e^{\mathbf{A}T_s} - \mathbf{I}\right)\mathbf{B} = \mathbf{A}^{-1}\left(\mathbf{I} + \mathbf{A}T_s - \mathbf{I}\right)\mathbf{B} = \mathbf{B}T_s. \tag{22}$$

Now to ensure guaranteed dominant pole placement depending on the pole placement parameter *m*, the system while neglecting the dynamics of non-dominant pole would behave like a second order system [6] with specified closed loop damping and natural frequency $\{\zeta_{cl}, \omega_{cl}\}$. Now using equation (22), the discretized form of equation (8) can be expressed as (23):

$$\mathbf{G} = \begin{bmatrix} 1 & T_s & 0 \\ 0 & 1 & T_s \\ 0 & -\left(\frac{T_s}{\tau^2}\right) & 1 - \frac{2\zeta_{ol}T_s}{\tau} \end{bmatrix}, \mathbf{H} = \begin{bmatrix} 0 \\ 0 \\ -\frac{KT_s}{\tau^2} \end{bmatrix}. \tag{23}$$

To design the discrete time optimal state feedback controller the standard infinite horizon quadratic cost (24) needs to be minimized, i.e.

$$J_d = \sum_{k=0}^{\infty} \mathbf{x}^T(k)\mathbf{Q}\mathbf{x}(k) + u^T(k)\mathbf{R}u(k). \tag{24}$$

The solution of the DARE can be obtained to minimize the quadratic cost (24) and is given by (25):

$$\mathbf{P} = \mathbf{G}^T\mathbf{P}\mathbf{G} - \mathbf{G}^T\mathbf{P}\mathbf{H}\left(\mathbf{H}^T\mathbf{P}\mathbf{H} + \mathbf{R}\right)^{-1}\mathbf{H}^T\mathbf{P}\mathbf{G} + \mathbf{Q}. \tag{25}$$

In equation (25), the Riccati solution and weights $\{\mathbf{P}, \mathbf{Q}, \mathbf{R}\}$ are in the same form as of the continuous time cases in equation (12), (13). Similar to the earlier continuous time treatment, the discrete time optimal state feedback controller gain matrix $\mathbf{K_s}$ can be achieved as (26) using the matrix $\mathbf{P}$ that minimizes the discrete quadratic cost function (24). Therefore we have:

$$\mathbf{K_s} = \left(\mathbf{H}^T\mathbf{P}\mathbf{H} + \mathbf{R}\right)^{-1}\mathbf{H}^T\mathbf{P}\mathbf{G}. \tag{26}$$

This gives the control law as (27):

$$u(k) = -\mathbf{K_s}\mathbf{x}(k). \tag{27}$$

Using (23) in (26) the discrete time state feedback gain can be obtained as (28):

$$\mathbf{K_s} = \left(\begin{bmatrix} 0 & 0 & -\frac{KT_s}{\tau^2} \end{bmatrix} \begin{bmatrix} P_{11} & P_{12} & P_{13} \\ P_{12} & P_{22} & P_{23} \\ P_{13} & P_{23} & P_{33} \end{bmatrix} \begin{bmatrix} 0 \\ 0 \\ -\frac{KT_s}{\tau^2} \end{bmatrix} + R \right)^{-1} \begin{bmatrix} 0 & 0 & -\frac{KT_s}{\tau^2} \end{bmatrix} \begin{bmatrix} P_{11} & P_{12} & P_{13} \\ P_{12} & P_{22} & P_{23} \\ P_{13} & P_{23} & P_{33} \end{bmatrix} \begin{bmatrix} 1 & T_s & 0 \\ 0 & 1 & T_s \\ 0 & -\left(\frac{T_s}{\tau^2}\right) & 1-\frac{2\zeta_{ol}T_s}{\tau} \end{bmatrix}$$

$$= -\left(-\frac{KT_s}{\tau^2} \begin{bmatrix} \widetilde{P_{13}} & \widetilde{P_{23}} & \widetilde{P_{33}} \end{bmatrix} \begin{bmatrix} 0 \\ 0 \\ -\frac{KT_s}{\tau^2} \end{bmatrix} + \widetilde{R} \right)^{-1} \frac{KT_s}{\tau^2} \begin{bmatrix} \widetilde{P_{13}} & \widetilde{P_{23}} & \widetilde{P_{33}} \end{bmatrix} \begin{bmatrix} 1 & T_s & 0 \\ 0 & 1 & T_s \\ 0 & -\left(\frac{T_s}{\tau^2}\right) & 1-\frac{2\zeta_{ol}T_s}{\tau} \end{bmatrix}$$

$$\Rightarrow \widetilde{\mathbf{K_s}} = -\begin{bmatrix} \widetilde{K_i} & \widetilde{K_p} & \widetilde{K_d} \end{bmatrix}. \tag{28}$$

Using the approach as mentioned above the discrete time PID controller gains $\{K_i, K_p, K_d\}$ can be obtained similar to the continuous time gains $\{K_i, K_p, K_d\}$ in (19) using discretized form of the actual system characteristic equation (17) and desired closed loop system characteristic equation (18). Again from (28) the discrete time PID controller gains $\{K_i, K_p, K_d\}$ can be represented as (29):

$$\left.\begin{aligned} K_i &= \frac{P_{13}KT_s\tau^2}{\left(P_{33}K^2T_s^2 + R\tau^4\right)} \\ K_p &= \frac{KT_s\left(P_{13}T_s\tau^2 + P_{23}\tau^2 - P_{33}T_s\right)}{\left(P_{33}K^2T_s^2 + R\tau^4\right)} \\ K_d &= \frac{KT_s\tau\left(P_{23}T_s\tau + P_{33}\tau - 2P_{33}\zeta_{ol}T_s\right)}{\left(P_{33}K^2T_s^2 + R\tau^4\right)} \end{aligned}\right\}. \tag{29}$$

The values of discrete time Riccati solution matrix elements $\{P_{33}, P_{23}, P_{13}\}$ can be calculated from equation (29) and takes the form as shown in (30):

$$\left.\begin{aligned} P_{33} &= \frac{R\tau^4\left(-K_p + K_iT_s + K_dT_s^{-1}\right)}{K\left[KK_pT_s^2 + T_s^2 - T_s^3KK_i - T_sKK_d + \tau^2 - 2\zeta_{ol}\tau T_s\right]} \\ P_{23} &= \left(P_{33}\left(K^2K_dT_s^2 - K\tau^2T_s + 2\zeta_{ol}\tau KT_s^2\right) + K_dR\tau^4\right)\Big/K\tau^2T_s^2 \\ P_{13} &= \left(K_i\left(P_{33}K^2T_s^2 + R\tau^4\right)\right)\Big/K\tau^2T_s \end{aligned}\right\}. \tag{30}$$

This implies that the elements of the **P** matrix can be derived from the given open loop and desired closed loop system parameters $\{K, \tau, \zeta_{ol}, m, \zeta_{cl}, \omega_{cl}\}$ using (19) as:

$$\left.\begin{aligned}
P_{33} &= \frac{R\tau^4\left[-\left(1+2m\zeta_{cl}^2\right)\tau^2 T_s\omega_{cl}^2 + T_s + m\zeta_{cl}\omega_{cl}^3\tau^2 T_s^2 + \left(2+m\right)\tau^2\zeta_{cl}\omega_{cl} - 2\zeta_{ol}\tau\right]}{K^2 T_s\left[T_s^2\left(\left(1+2m\zeta_{cl}^2\right)\tau^2\omega_{cl}^2 - m\zeta_{cl}\omega_{cl}^3\tau^2 T_s\right) - T_s\left(\left(2+m\right)\zeta_{cl}\omega_{cl}\tau^2 - 2\zeta_{ol}\tau\right) + \tau^2 - 2\zeta_{ol}\tau T_s\right]} \\
P_{23} &= \frac{P_{33}\left(K^2 T_s\left(\left(2+m\right)\zeta_{cl}\omega_{cl}\tau^2 T_s - 2\zeta_{ol}\tau T_s - \tau^2 + 2\zeta_{ol}\tau T_s\right)\right) + R\tau^4\left(\left(2+m\right)\zeta_{cl}\omega_{cl}\tau^2 - 2\zeta_{ol}\tau\right)}{K^2\tau^2 T_s^2} \\
\widetilde{P_{13}} &= \frac{m\zeta_{cl}\omega_{cl}^3\tau^2\left(\widetilde{P_{33}K^2 T_s^2} + \widetilde{R\tau^4}\right)}{K^2\tau^2 T_s}
\end{aligned}\right\}. \quad (31)$$

The diagonal elements of $\mathbf{Q}$ matrix can be obtained with the help of equation (19), (23), (25)-(30) and are shown in equation (32):

$$\left.\begin{aligned}
Q_{11} &= P_{13}K_i K T_s/\tau^2 \\
Q_{22} &= \left(-P_{11}\tau^4 T_s^2 - 2P_{12}\tau^4 T_s + \tau^2\left(2+KK_p\right)\left(P_{13}T_s^2 + P_{23}T_s\right) - P_{33}T_s^2\left(1+KK_p\right)\right)/\tau^4 \\
Q_{33} &= \left(-P_{22}\tau^3 T_s^2 + P_{23}\tau T_s\left(4\zeta_{ol}\tau T_s - 2\tau^2 + KK_d T_s\right) + P_{33}T_s\left(2\zeta_{ol}\tau^2 + \left(\tau - 2\zeta_{ol}T_s\right)\left(2\zeta_{ol}\tau + KK_d\right)\right)\right)/\tau^3
\end{aligned}\right\}. \quad (32)$$

Now using (28)-(30) the diagonal elements of $\mathbf{Q}$ matrix can be written in expanded form by replacing the expressions of the PID controller gains from (29) as shown in (33):

$$\begin{aligned}
Q_{11} &= P_{13}^2 K^2 T_s^2/\left(P_{33}K^2 T_s^2 + R\tau^4\right) \\
Q_{22} &= \frac{\left[\begin{array}{l}\left(-P_{11}\tau^4 T_s^2 - 2P_{12}\tau^4 T_s\right)\left(P_{33}K^2 T_s^2 + R\tau^4\right) + \\ \tau^2\left(2\left(P_{33}K^2 T_s^2 + R\tau^4\right) + K^2 T_s\left(P_{13}\tau^2 T_s + P_{23}\tau^2 - P_{33}T_s\right)\right)\left(P_{13}T_s^2 + P_{23}T_s\right) \\ -P_{33}T_s^2\left(\left(P_{33}K^2 T_s^2 + R\tau^4\right) + K^2 T_s\left(P_{13}\tau^2 T_s + P_{23}\tau^2 - P_{33}T_s\right)\right)\end{array}\right]}{\left(\tau^4\left(P_{33}K^2 T_s^2 + R\tau^4\right)\right)} \\
Q_{33} &= \frac{\left[\begin{array}{l}-P_{22}\tau^3 T_s^2\left(P_{33}K^2 T_s^2 + \widetilde{R\tau^4}\right) \\ +\widetilde{P_{23}\tau}T_s\left(\left(4\zeta_{ol}\tau T_s - 2\tau^2\right)\left(\widetilde{P_{33}K^2 T_s^2} + \widetilde{R\tau^4}\right) + K^2\tau T_s^2\left(\widetilde{P_{23}\tau}T_s + \widetilde{P_{33}\left(\tau - 2\zeta_{ol}T_s\right)}\right)\right) \\ +\widetilde{P_{33}T_s}\left(2\zeta_{ol}\tau^2\left(\widetilde{P_{33}K^2 T_s^2} + \widetilde{R\tau^4}\right) + \left(\tau - 2\zeta_{ol}T_s\right)\left(2\zeta_{ol}\tau\left(\widetilde{P_{33}K^2 T_s^2} + \widetilde{R\tau^4}\right) + K^2\tau T_s\left(\widetilde{P_{23}\tau}T_s + \widetilde{P_{33}\left(\tau - 2\zeta_{ol}T_s\right)}\right)\right)\right)\end{array}\right]}{\left(\tau^3\left(\widetilde{P_{33}K^2 T_s^2} + \widetilde{R\tau^4}\right)\right)}.
\end{aligned} \quad (33)$$

From the off-diagonal elements $\left\{Q_{12}, Q_{13}, Q_{23}\right\}$ of $\mathbf{Q}$ which is assumed to be zero and using $\mathbf{P} = \mathbf{P}^T$, the elements $\left\{P_{11}, P_{12}, P_{22}\right\}$ of $\mathbf{P}$ matrix can be derived using the equation (19), (23), (25)-(30) as shown in equation (34):

$$
\left.
\begin{aligned}
P_{11} &= P_{13}\left(1+KK_p\right)\big/\tau^2 = P_{13}\left(\left(P_{33}K^2T_s^2+R\tau^4\right)+K^2T_s\left(P_{13}\tau^2T_s+\tilde{P}_{23}\tau^2-P_{33}T_s\right)\right)\big/\left(\tau^2\left(P_{33}K^2T_s^2+R\tau^4\right)\right)\\
P_{12} &= P_{13}\left(2\zeta_{ol}\tau+KK_d\right)\big/\tau^2 = \frac{P_{13}\left(2\zeta_{ol}\tau\left(P_{33}K^2T_s^2+R\tau^4\right)+K^2\tau T_s\left(P_{23}\tau T_s+P_{33}\left(\tau-2\zeta_{ol}T_s\right)\right)\right)}{\left(\tau^2\left(P_{33}K^2T_s^2+R\tau^4\right)\right)}\\
P_{22} &= \left(-P_{12}\tau^4T_s+P_{23}\tau^2\left(KK_d+T_s+2\zeta_{ol}\tau\right)+P_{13}\tau^2\left(2\zeta_{ol}\tau T_s-\tau^2+KK_dT_s\right)+P_{33}\left(\tau^2-2\zeta_{ol}\tau T_s-K\widetilde{K_dT_s}\right)\right)\big/\tau^4\\
&= \frac{\left[\begin{array}{l}
-\widetilde{P_{12}\tau^4}T_s\left(\widetilde{P_{33}K^2}T_s^2+\widetilde{R\tau^4}\right)+\widetilde{P_{23}\tau^2}\left(K^2T_s\tau\left(\widetilde{P_{23}\tau}T_s+\widetilde{P_{33}\left(\tau-2\zeta_{ol}T_s\right)}\right)+\left(T_s+2\zeta_{ol}\tau\right)\left(\widetilde{P_{33}K^2}T_s^2+\widetilde{R\tau^4}\right)\right)\\
+\widetilde{P_{13}\tau^2}\left(\left(2\zeta_{ol}\tau T_s-\tau^2\right)\left(\widetilde{P_{33}K^2}T_s^2+\widetilde{R\tau^4}\right)+K^2T_s^2\tau\left(\widetilde{P_{23}\tau}T_s+\widetilde{P_{33}\left(\tau-2\zeta_{ol}T_s\right)}\right)\right)\\
+\widetilde{P_{33}}\left(\left(\tau^2-2\zeta_{ol}\tau T_s\right)\left(\widetilde{P_{33}K^2}T_s^2+\widetilde{R\tau^4}\right)-K^2T_s^2\tau\left(\widetilde{P_{23}\tau}T_s+\widetilde{P_{33}\left(\tau-2\zeta_{ol}T_s\right)}\right)\right)
\end{array}\right]}{\tau^4\left(\widetilde{P_{33}K^2}T_s^2+\widetilde{R\tau^4}\right)}
\end{aligned}
\right\}. \tag{34}
$$

For this particular choice of $\mathbf{Q}$, there exists a DARE solution $\mathbf{P}$. The above transformation of $\mathbf{Q}$ in (32) and $\mathbf{Q}$ in (21) gives the new PID controller gains in discrete and continuous time respectively. The aim here is to closely match the continuous and discrete time PID controller gains ($\mathbf{K_s}$ and $\mathbf{K_s}$ respectively) and establishing the transformation between the respective LQR weights which produces minimal variation in the desired closed loop response, even with wide variation of the sampling time. It is also interesting to note that in the discrete time LQR, the weighting matrices (32) and the Riccati solution (30) and (34) both contain the sampling time T_s to match the optimality conditions from the continuous to discrete time conversion.

3. Continuous and discrete time PID controller tuning using dominant pole placement for first order integrating system with continuous/discrete time LQR

In this section the optimal continuous and discrete time PID controller design methodology have been extended for the first order integrating system as shown in Figure 1(b). The first order system with an integrator essentially makes the system second order. Thus, it is better to control this type of process using PID controller, instead of simple PI controller. The system can be represented as:

$$G_2(s) = K/s(\tau s+1). \tag{35}$$

It is seen that the open loop system $G_2(s)$ has two poles at the origin and $(-1/\tau)$. To design the PID controller using LQR method with the assumption of external set-point input $r(t)=0$, the corresponding state space model of (35) takes the form as:

$$\dot{x}_1 = x_2,\ \dot{x}_2 = x_3,\ \dot{x}_3 = -(1/\tau)x_3 - (K/\tau)u, \tag{36}$$

where $x_1 = \int_0^t e(\tau)d\tau,\ x_2 = e(t) = \dot{x}_1,\ x_3 = \dfrac{de(t)}{dt} = \dot{x}_2$.

Thus equation (36) is used to design the state space model in the form (7) where the system matrices are given in (37) as:

$$\mathbf{A}=\begin{bmatrix} 0 & 1 & 0 \\ 0 & 0 & 1 \\ 0 & 0 & -\dfrac{1}{\tau} \end{bmatrix},\mathbf{B}=\begin{bmatrix} 0 \\ 0 \\ -\dfrac{K}{\tau} \end{bmatrix},\mathbf{C}=\begin{bmatrix} 0 & 1 & 0 \end{bmatrix}. \tag{37}$$

Now, the closed loop transfer function of system (35) with a PID controller (2) can be represents as:

$$G_{2cl}(s)=\frac{C_1(s)G_2(s)}{1+C_1(s)G_2(s)}, \tag{38}$$

which yields the corresponding closed loop characteristic equation as (39), i.e.

$$\Delta_3(s)=s^3+\left(\frac{1+KK_d}{\tau}\right)s^2+\frac{KK_p}{\tau}s+\frac{KK_i}{\tau}=0. \tag{39}$$

Again, comparing coefficient of the desired closed loop characteristic equation (18) and closed loop characteristic equation with the controller (39), the three PID controller gains are obtained as (40):

$$\left.\begin{aligned} K_i &= m\zeta_{cl}\omega_{cl}^3\tau/K \\ K_p &= \left(1+2m\zeta_{cl}^2\right)\omega_{cl}^2\tau/K \\ K_d &= \left(\left(2+m\right)\zeta_{cl}\omega_{cl}\tau-1\right)/K \end{aligned}\right\}. \tag{40}$$

Now to design the LQR based continuous time PID controller the state feedback gain matrix $\mathbf{K_s}$ can be obtained in the form of PID controller gains using control law (10) as (41):

$$\mathbf{K_s}=\mathbf{R}^{-1}\begin{bmatrix} 0 & 0 & -\dfrac{K}{\tau} \end{bmatrix}\begin{bmatrix} P_{11} & P_{12} & P_{13} \\ P_{12} & P_{22} & P_{23} \\ P_{13} & P_{23} & P_{33} \end{bmatrix}=\mathbf{R}^{-1}\begin{bmatrix} -\dfrac{KP_{13}}{\tau} & -\dfrac{KP_{23}}{\tau} & -\dfrac{KP_{33}}{\tau} \end{bmatrix}=-\begin{bmatrix} K_i & K_p & K_d \end{bmatrix}. \tag{41}$$

Then the elements $\{P_{13},P_{23},P_{33}\}$ of $\mathbf{P}=\mathbf{P}^T$ matrix as in (12) can be represented in the form of PID controller gain or pole placement parameter, as well as the open loop and closed loop system parameters i.e. $\{m,K,\tau,\zeta_{cl},\omega_{cl}\}$ using (40)-(41) as:

$$\left.\begin{aligned} P_{13} &= R\tau K_i/K = R\tau^2 m\zeta_{cl}\omega_{cl}/K^2 \\ P_{23} &= R\tau K_p/K = R\tau^2\omega_{cl}^2\left(1+2m\zeta_{cl}^2\right)/K^2 \\ P_{33} &= R\tau K_d/K = R\tau\left(\zeta_{cl}\omega_{cl}\tau\left(2+m\right)-1\right)/K^2 \end{aligned}\right\}. \tag{42}$$

Assuming off-diagonal elements of $\mathbf{Q}$ matrix are zero as in (13), the diagonal elements of $\mathbf{Q}$ matrix and one element of $\mathbf{P}$ matrix i.e. P_{12} using (37), (40)-(42) and (10)-(13) yields:

$$\left.\begin{aligned} Q_{11} &= P_{13}KK_i/\tau = P_{13}m\zeta_{cl}\omega_{cl}^3 \\ Q_{22} &= \left(P_{23}KK_p - 2\tau P_{12}\right)\big/\tau = P_{23}\omega_{cl}^2\left(1+2m\zeta_{cl}^2\right) - 2P_{12} \\ Q_{33} &= \left(P_{33}\left(2+KK_d\right) - 2\tau P_{23}\right)\big/\tau = \left(P_{33}\left(1+\zeta_{cl}\omega_{cl}\tau\left(2+m\right)\right) - 2P_{23}\right)\big/\tau \end{aligned}\right\}, \tag{43}$$

and

$$P_{12} = P_{13}\left(1+KK_d\right)\big/\tau = P_{13}\zeta_{cl}\omega_{cl}\left(2+m\right). \tag{44}$$

Thus using (43), the $\mathbf{Q}$ matrix can be designed in the form of (13) which is used to obtain the continuous time PID controller gain from CARE (11) considering fixed weighting factor *R*.

As discussed in the previous section, for designing the digital PID controller for the system (37), the system matrix (37) is discretized with sampling time T_s and using (22) the corresponding discrete time state space model is:

$$\mathbf{G} = \begin{bmatrix} 1 & T_s & 0 \\ 0 & 1 & T_s \\ 0 & 0 & 1-\dfrac{T_s}{\tau} \end{bmatrix}, \mathbf{H} = \begin{bmatrix} 0 \\ 0 \\ -\dfrac{KT_s}{\tau} \end{bmatrix}. \tag{45}$$

Therefore the discrete time state feedback gain matrix $\left(\mathbf{K_s}\right)$ can be obtained using (45) and (26) as:

$$\begin{aligned} \mathbf{K_s} &= \left(\begin{bmatrix} 0 & 0 & -\dfrac{KT_s}{\tau} \end{bmatrix} \begin{bmatrix} P_{11} & P_{12} & P_{13} \\ P_{12} & P_{22} & P_{23} \\ P_{13} & P_{23} & P_{33} \end{bmatrix} \begin{bmatrix} 0 \\ 0 \\ -\dfrac{KT_s}{\tau} \end{bmatrix} + R \right)^{-1} \begin{bmatrix} 0 & 0 & -\dfrac{KT_s}{\tau} \end{bmatrix} \begin{bmatrix} P_{11} & P_{12} & P_{13} \\ P_{12} & P_{22} & P_{23} \\ P_{13} & P_{23} & P_{33} \end{bmatrix} \begin{bmatrix} 1 & T_s & 0 \\ 0 & 1 & T_s \\ 0 & 0 & 1-\dfrac{T_s}{\tau} \end{bmatrix} \\ &= -\left(-\frac{KT_s}{\tau}\begin{bmatrix} P_{13} & P_{23} & P_{33} \end{bmatrix} \begin{bmatrix} 0 \\ 0 \\ -\dfrac{KT_s}{\tau} \end{bmatrix} + \widetilde{R} \right)^{-1} \frac{KT_s}{\tau}\begin{bmatrix} \widetilde{P_{13}} & \widetilde{P_{23}} & \widetilde{P_{33}} \end{bmatrix} \begin{bmatrix} 1 & T_s & 0 \\ 0 & 1 & T_s \\ 0 & 0 & 1-\dfrac{T_s}{\tau} \end{bmatrix} \\ \Rightarrow \widetilde{\mathbf{K_s}} &= -\begin{bmatrix} \widetilde{K_i} & \widetilde{K_p} & \widetilde{K_d} \end{bmatrix}. \end{aligned} \tag{46}$$

Using a similar approach as shown in the previous section the discrete time PID controller gains $\left\{K_i, K_p, K_d\right\}$ can be obtained similar to the continuous time gains $\left\{K_i, K_p, K_d\right\}$ in (40) using discretized form of the actual closed loop system characteristic equation (39) and the desired closed loop system characteristic equation (18). From (46) the discrete time PID controller gain $\left\{K_i, K_p, K_d\right\}$ can be obtained as (47), i.e.

$$\left.\begin{aligned} K_i &= \frac{K P_{13} T_s \tau}{\left(P_{33} K^2 T_s^2 + R\tau^2\right)} \\ K_p &= \frac{K T_s \tau \left(P_{13} T_s + P_{23}\right)}{\left(P_{33} K^2 T_s^2 + R\tau^2\right)} \\ K_d &= \frac{P_{23} K^2 T_s^2 \tau + \left(\tau - T_s\right) P_{33} K T_s}{\left(P_{33} K^2 T_s^2 + R\tau^2\right)} \end{aligned}\right\}. \tag{47}$$

However, using (47) the elements of $\mathbf{P} = \mathbf{P}^T$ matrix i.e. $\left\{P_{13}, P_{23}, P_{33}\right\}$ can be represented as (48):

$$\left.\begin{aligned} P_{33} &= -\frac{R\tau^3 \left(K_d - K_p T_s + K_i T_s^2\right)}{K\tau T_s \left(K T_s \left(K_d - K_p T_s + K_i T_s^2\right) - \tau + T_s\right)} \\ P_{13} &= \frac{K_i \left(P_{33} K^2 T_s^2 + R\tau^2\right)}{K\tau T_s} \\ P_{23} &= P_{13}\left(\frac{K_p}{K_i} - T_s\right) \end{aligned}\right\}. \tag{48}$$

Again, equation (48) can be rewritten in terms of the pole placement, open loop and closed loop system parameters $\left\{m, K, \tau, \zeta_{cl}, \omega_{cl}\right\}$ as:

$$\left.\begin{aligned} P_{33} &= \frac{R\tau^2 \left[\zeta_{cl}\omega_{cl}\tau\left(2+m\right) - 1 - \tau T_s \left(\omega_{cl}^2 \left(1 + 2m\zeta_{cl}^2\right) - m\zeta_{cl}\omega_{cl}^3 T_s\right)\right]}{K^2 T_s \left[\tau - T_s - T_s\left(\zeta_{cl}\omega_{cl}\tau\left(2+m\right) - 1\right) + \tau T_s^2 \left(\omega_{cl}^2 \left(1 + 2m\zeta_{cl}^2\right) - m\zeta_{cl}\omega_{cl}^3 T_s\right)\right]} \\ P_{13} &= \frac{m\zeta_{cl}\omega_{cl}^3 \left(P_{33} K^2 T_s^2 + R\tau^2\right)}{K^2 T_s} \\ P_{23} &= \frac{\left(P_{33} K^2 T_s^2 + R\tau^2\right)\left(\omega_{cl}^2 \left(1 + 2m\zeta_{cl}^2\right) - m\zeta_{cl}\omega_{cl}^3 T_s\right)}{K^2 T_s} \end{aligned}\right\}. \tag{49}$$

Now, defining $\mathbf{Q}$ matrix as in (13) where the off-diagonal elements are assumed to be zero and using (25)-(26), (45), (47)-(49), the rest of the elements $\left\{P_{11}, P_{12}, P_{22}\right\}$ of $\mathbf{P}$ matrix and the diagonal elements of $\mathbf{Q}$ matrix can be obtained as:

$$\left.\begin{aligned}
P_{11} &= \frac{P_{13}KK_p}{\tau} = \frac{K^2T_sP_{13}\left(P_{13}T_s+P_{23}\right)}{\left(P_{33}K^2T_s^2+R\tau^2\right)} \\
P_{12} &= \frac{P_{13}\left(1+KK_d\right)}{\tau} = \frac{K^2\tau T_sP_{13}\left(P_{23}T_s+\left(1-\frac{T_s}{\tau}\right)P_{23}\right)+P_{13}}{\tau\left(P_{33}K^2T_s^2+R\tau^2\right)} \\
P_{22} &= \frac{KK_d\left(P_{13}T_s+P_{23}\right)}{\tau}-P_{12}T_s-\left(1-\frac{T_s}{\tau}\right)P_{13}+\frac{P_{23}}{\tau} \\
&= \frac{K^2T_s\left(P_{13}T_s+P_{23}\right)\left(P_{23}T_s+\left(1-\frac{T_s}{\tau}\right)P_{23}\right)}{\left(P_{33}K^2T_s^2+R\tau^2\right)}-\widetilde{P_{12}T_s}-\left(1-\frac{T_s}{\tau}\right)\widetilde{P_{13}}+\widetilde{\frac{P_{23}}{\tau}}
\end{aligned}\right\}, \tag{50}$$

and

$$\left.\begin{aligned}
Q_{11} &= \frac{P_{13}KK_iT_s}{\tau} = \frac{\left(P_{13}KT_s\right)^2}{\left(P_{33}K^2T_s^2+R\tau^2\right)} \\
Q_{22} &= \frac{KK_pT_s\left(P_{13}T_s+P_{23}\right)}{\tau}-P_{11}T_s^2-2P_{12}T_s = \frac{K^2T_s^2\left(P_{13}T_s+P_{23}\right)^2}{\left(P_{33}K^2T_s^2+R\tau^2\right)}-P_{11}T_s^2-2P_{12}T_s \\
Q_{33} &= \frac{P_{23}T_s\tau\left(KK_dT_s-2\left(\tau-T_s\right)\right)+P_{33}\left(KK_dT_s\left(\tau-T_s\right)+2\tau T_s-T_s^2\right)-P_{22}T_s^2\tau^2}{\tau^2} \\
&= \frac{K^2T_s^2\left(P_{23}T_s+\left(1-\frac{T_s}{\tau}\right)P_{33}\right)^2}{\left(P_{33}K^2T_s^2+\widetilde{R\tau^2}\right)}-\widetilde{P_{22}T_s^2}-2\widetilde{P_{23}T_s}\left(1-\frac{T_s}{\tau}\right)+\widetilde{P_{33}}\left(1-\left(1-\frac{T_s}{\tau}\right)^2\right)
\end{aligned}\right\}. \tag{51}$$

The DARE can be used to obtain digital PID controller gains with designed $\mathbf{Q}$ matrix using (51) and fixed R for the system (35).

4. Continuous and discrete time PI controller tuning using pole placement for a first order system with continuous/discrete time LQR

Here, the same design methodology has been extended for an optimal discrete PID controller considering a first order system controlled by a PI controller as shown in Figure 1(c). It is a well-known fact that to control a first order process, a PI controller is sufficient without the need of a derivative action. The first order system can be represented as:

$$G_3(s) = K/(\tau s+1), \tag{52}$$

which is to be controlled by the PI controller (53):

$$C_3(s) = K_p+\frac{K_i}{s}, \tag{53}$$

where, $\{K_i, K_p\}$ are the integral and proportional gains of the PI controller.

The transfer function $G_3(s)$ in equation (52) represents open loop system with its pole lying at $(-1/\tau)$ with DC gain K. To formulate LQR controller, the external set point $r(t)$ is assumed to be zero as it does not affect the controller design result, previously shown in [19].

So the state space model can be formulated in the same way and given in (54), i.e.

$$\dot{x}_1 = x_2, \dot{x}_2 = -\frac{x_2}{\tau} - \frac{K}{\tau}u(t), \tag{54}$$

where, $x_1 = \int_0^t e(\tau)d\tau, x_2 = e(t) = \dot{x}_1$.

Using (54) the state space model of the system (52) with the augmented state $\mathbf{x}(t) = \begin{bmatrix} x_1(t) & x_2(t) \end{bmatrix}^T$ can be represented as (7) and the corresponding system matrices are given by:

$$\mathbf{A} = \begin{bmatrix} 0 & 1 \\ 0 & -\frac{1}{\tau} \end{bmatrix}, \mathbf{B} = \begin{bmatrix} 0 \\ -\frac{K}{\tau} \end{bmatrix}, \mathbf{C} = \begin{bmatrix} 0 & 1 \end{bmatrix}. \tag{55}$$

Again, the closed loop transfer function for the system (52) with a PI controller (53) can be represents as:

$$G_{3cl}(s) = \frac{\left(K_p + \frac{K_i}{s}\right)G_3(s)}{1 + \left(K_p + \frac{K_i}{s}\right)G_3(s)}. \tag{56}$$

The corresponding characteristic equation of the above closed loop system will be:

$$\Delta_4(s) = s^2\tau + (1 + KK_p)s + KK_i = 0. \tag{57}$$

As (57) has two roots in the left half of the *s*-plane, the desired closed loop characteristic equation can be expressed as:

$$\Delta_5(s) = s^2 + 2\xi_{cl}\omega_{cl}s + \omega_{cl}^2 = 0. \tag{58}$$

It is to be noted that for the control of first order system, since the resulting characteristic equation with PI controller is of second order, it does not need a dominant pole placement formulation. Rather a simpler pole placement formulation where one does not need to consider about the non-dominant pole, can be adopted as in the case of second order and first order integrating processes.

Now matching the co-efficient of equation (57) and (58), the PI controller gains can be obtained as:

$$\left.\begin{aligned} K_i &= \frac{\omega_{cl}^2 \tau}{K} \\ K_p &= \frac{2\zeta_{cl}\omega_{cl}\tau - 1}{K} \end{aligned}\right\}. \tag{59}$$

To design LQR based continuous time optimal PI controller the cost function, state feedback gain and the Riccati equation can be represented as the same way in (9)-(11). Also, the $\{\mathbf{P},\mathbf{Q},\mathbf{R}\}$ matrices can be expressed in the general form as (60) of appropriate dimension, i.e.

$$\mathbf{P} = \begin{bmatrix} P_{11} & P_{12} \\ P_{21} & P_{22} \end{bmatrix}, \mathbf{Q} = \begin{bmatrix} Q_{11} & Q_{12} \\ Q_{21} & Q_{22} \end{bmatrix} = \begin{bmatrix} Q_{11} & 0 \\ 0 & Q_{22} \end{bmatrix}, \mathbf{R} = 1. \tag{60}$$

Using the equations (10), (55), (60), the continuous time state feedback gain matrix is derived as:

$$\mathbf{K_s} = \mathbf{R}^{-1}\begin{bmatrix} 0 & -\frac{K}{\tau} \end{bmatrix}\begin{bmatrix} P_{11} & P_{12} \\ P_{12} & P_{22} \end{bmatrix} = -\frac{K}{R\tau}\begin{bmatrix} P_{12} & P_{22} \end{bmatrix} = -\begin{bmatrix} K_i & K_p \end{bmatrix}. \tag{61}$$

The elements $\{P_{12}, P_{22}\}$ of the $\mathbf{P}$ matrix can be calculated from equation (59) and (61) in the form:

$$\left.\begin{aligned} P_{12} &= \frac{K_i R\tau}{K} = \frac{R\tau^2\omega_{cl}^2}{K^2} \\ P_{22} &= \frac{K_p R\tau}{K} = \frac{R\tau\left(2\zeta_{cl}\omega_{cl}\tau - 1\right)}{K^2} \end{aligned}\right\}. \tag{62}$$

Using the property of $\mathbf{P} = \mathbf{P}^T$, the diagonal elements of $\mathbf{Q}$ matrix can be derived in (63), while considering the off-diagonal elements being zero with the help of equations (10), (11), (55), (59)-(62) as:

$$\left.\begin{aligned} Q_{11} &= \frac{P_{12}KK_i}{\tau} = \frac{P_{12}^2K^2}{R\tau^2} \\ Q_{22} &= P_{22}\left(\frac{2}{\tau} + \frac{KK_p}{\tau}\right) - 2P_{12} = \frac{P_{22}^2K^2}{R\tau^2} - 2\left(P_{12} - \frac{P_{22}}{\tau}\right) \end{aligned}\right\}. \tag{63}$$

Using the off-diagonal element $Q_{12} = 0$, the element P_{11} of $\mathbf{P}$ matrix can be derived using the equations (10), (11), (55), (61)-(62) as:

$$P_{11} = P_{12}\left(\frac{1 + KK_p}{\tau}\right) = \left(\frac{P_{12}}{\tau} + \frac{P_{12}P_{22}K^2}{R\tau^2}\right). \tag{64}$$

Now, to design a digital PID controller, the discretized form of system matrix (55) can be obtained using the sampling time T_s and thus equation (22) can be expressed as:

$$\mathbf{G} = \begin{bmatrix} 1 & T_s \\ 0 & 1 - (T_s/\tau) \end{bmatrix}, \mathbf{H} = \begin{bmatrix} 0 \\ -(KT_s/\tau) \end{bmatrix}. \tag{65}$$

The discrete time state feedback gain $\mathbf{K_s}$ for the PI controller with discrete LQR can be obtained using equations (26), (60), (65) in the following form:

$$\begin{aligned}\mathbf{K_s} &= \left(\begin{bmatrix} 0 & -\left(KT_s/\tau\right) \end{bmatrix} \begin{bmatrix} P_{11} & P_{12} \\ P_{12} & P_{22} \end{bmatrix} \begin{bmatrix} 0 \\ -\left(KT_s/\tau\right) \end{bmatrix} + R \right)^{-1} \begin{bmatrix} 0 & -\left(KT_s/\tau\right) \end{bmatrix} \begin{bmatrix} P_{11} & P_{12} \\ P_{12} & P_{22} \end{bmatrix} \begin{bmatrix} 1 & T_s \\ 0 & 1-\left(T_s/\tau\right) \end{bmatrix} \\ &= \left(\frac{P_{22}K^2T_s^2}{\tau^2} + \tilde{R} \right)^{-1} \begin{bmatrix} -\frac{P_{12}KT_s}{\tau} & -\left(P_{12}T_s + P_{22} - \frac{P_{22}T_s}{\tau} \right) \frac{KT_s}{\tau} \end{bmatrix} \\ \Rightarrow \mathbf{K_s} &= -\begin{bmatrix} K_i & K_p \end{bmatrix}. \end{aligned} \tag{66}$$

Then from (66) the discrete time PI controller gains $\left\{K_i, K_p\right\}$ can be obtained as:

$$\left.\begin{aligned} K_i &= \frac{P_{12}KT_s\tau}{\left(P_{22}K^2T_s^2 + R\tau^2\right)} \\ K_p &= \frac{\left(P_{12}T_s\tau + P_{22}\left(\tau - T_s\right)\right)KT_s}{\left(P_{22}K^2T_s^2 + R\tau^2\right)} \end{aligned}\right\}. \tag{67}$$

A similar approach as mentioned in the previous section can be obtained for deriving the discrete time PI controller gains $\left\{K_i, K_p\right\}$ corresponding to the continuous time gains $\left\{K_i, K_p\right\}$ as in (59) using discretized form of the closed loop system characteristic equation (57) and the desired closed loop system characteristic equation (58). The elements $\left\{P_{12}, P_{22}\right\}$ of $\mathbf{P}$ matrix can be derived with the help of equation (66) and (59) and given as:

$$\left.\begin{aligned} P_{22} &= \frac{R\tau^2\left(K_iT_s - K_p\right)}{\left(K_pK^2T_s^2 - \left(\tau - T_s\right)KT_s - K_iK^2T_s^3\right)} = \frac{R\tau^2\left(\omega_{cl}^2\tau T_s - 2\zeta_{cl}\omega_{cl}\tau + 1\right)}{K^2T_s\left(\left(2\zeta_{cl}\omega_{cl}\tau - 1\right)T_s - \tau + T_s - \omega_{cl}^2\tau T_s^2\right)} \\ P_{12} &= \frac{\tilde{K}_i}{K\tau T_s}\left(P_{22}K^2T_s^2 + R\tau^2\right) = \frac{\omega_{cl}^2}{K^2T_s}\left(P_{22}K^2T_s^2 + R\tau^2\right) \end{aligned}\right\}. \tag{68}$$

The diagonal elements $\left\{Q_{11}, Q_{22}\right\}$ of the weighting matrix $\mathbf{Q}$ using equation (25), (60), (65)-(68) are obtained as:

$$\left.\begin{aligned} Q_{11} &= P_{12}KK_iT_s/\tau = \frac{P_{12}^2K^2T_s^2}{\left(P_{22}K^2T_s^2 + R\tau^2\right)} \\ Q_{22} &= \frac{-P_{11}\tau^2T_s^2 + P_{12}\tau T_s\left(2\left(T_s - \tau\right) + T_sKK_p\right) + P_{22}T_s\left(\tau\left(2 + KK_p\right) - T_s\left(1 + KK_p\right)\right)}{\tau^2} \\ &= \frac{\left(P_{22}K^2T_s^2 + R\tau^2\right)\left(-P_{11}\tau^2T_s^2 + 2P_{12}T_s\tau\left(T_s - \tau\right) + P_{22}T_s\left(2\tau - T_s\right)\right) + K^2T_s^2\left(P_{12}\tau T_s + P_{22}\left(\tau - T_s\right)\right)^2}{\tau^2\left(P_{22}K^2T_s^2 + R\tau^2\right)} \end{aligned}\right\}. \tag{69}$$

Moreover, P_{11} can be derived in (70) by setting the off-diagonal element Q_{12} of weighting matrix $\mathbf{Q}$ to zero. Therefore we have:

$$P_{11} = \frac{P_{12}}{\tau}\left(1 + KK_p\right) = \frac{P_{12}\left(P_{22}K^2\tau T_s + K^2T_s^2P_{12}\tau + R\tau^2\right)}{\tau\left(P_{22}K^2T_s^2 + R\tau^2\right)}. \tag{70}$$

The equation (68) and (70) result in the transformed $\mathbf{Q}$ matrix (69) based on discrete time LQR approach which yields state feedback controller gains K_s to get approximately close time domain characteristics to the original continuous time system (52).

5. Simulation examples

5.1. Test-bench systems

The utility of the proposed transformations of discrete time LQR weight ($\mathbf{Q}$) has now been tested for three classes of systems including second order, first order integrating and first order system in the following subsections. These three classes of models are chosen since they represent a wide variety of processes in industrial control applications. In fact, many higher order systems can effectively be reduced or identified in these templates from real process operation data.

Three second order stable processes (71)-(73) are first chosen as shown in [30], where the first two exhibits undamped and the third one show a critically damped open loop dynamics, i.e.

$$G_1(s) = \frac{1}{\left(s^2 + 1\right)}, \tag{71}$$

$$G_2(s) = \frac{1}{\left(s^2 + 36\right)}, \tag{72}$$

$$G_3(s) = \frac{1}{\left(s + 0.2\right)^2}. \tag{73}$$

Next a second order repeated pole critically damped process has been chosen from [31] as these has been used as test cases by controller manufacturers like Eurotherm and Foxboro and is given by:

$$G_4(s) = \frac{1}{\left(s + 1\right)^2}. \tag{74}$$

A second order overdamped test-bench process (75) is given in [32] as:

$$G_5(s) = \frac{1}{\left(1 + 0.2s\right)\left(1 + s\right)}. \tag{75}$$

Now, a second order process with two unstable poles can be found in [30] is also included in the test-bench and is given by:

$$G_6(s) = \frac{1}{\left(s - 0.2\right)^2}. \tag{76}$$

Two second order processes with one stable and one unstable pole can be found in [33] and also with two unstable poles as in [31], the latter representing an inverted pendulum or an unstable batch reactor i.e.

$$G_7(s) = \frac{4}{(s+4)(s-1)}, \tag{77}$$

$$G_8(s) = \frac{1}{(s^2-1)}. \tag{78}$$

It is clear that the processes G_7-G_8 under control have real coefficients. However, when casting them in the standard second order template, the time constants and damping can be an imaginary number, especially for the second order unstable systems. This essentially suggest that the open-loop unstable processes cannot be represented in second order template with real-valued time constant and damping, otherwise it may turn out to be imaginary.

Therefore, we have eight second order processes exhibiting various stable and unstable open loop dynamics which can be casted as the same model template (1), where the respective DC gains, time constants and damping ratios are reported in Table 1.

Table 1: Test-bench processes with their open and closed loop parameters and maximum allowable sampling time to closed-loop time constant ratio (T_s/τ_{cl})

Class of systems	**Process model**	K	τ	ζ_{ol}	ω_{cl}	$\tau_{cl} = 1/\omega_{cl}$	T_s	***Maximum allowable*** T_s/τ_{cl}
	$G_1 = 1/(s^2+1)$	1	1	0	10	0.1	0.05	0.5
	$G_2 = 1/(s^2+36)$	1/36	1/6	0	10	0.1	0.05	0.5
	$G_3 = 1/(s+0.2)^2$	25	5	1	10	0.1	0.05	0.5
	$G_4 = 1/(s+1)^2$	1	1	1	10	0.1	0.05	0.5
SO stable	$G_5 = 1/((1+0.2s)(1+s))$	1	0.4472	1.3416	10	0.1	0.05	0.5
	$G_6 = 1/(s-0.2)^2$	25	5	-1	10	0.1	0.05	0.5
	$G_7 = 4/(s+4)(s-1)$	-1	$0.5j$	$0.75j$	10	0.1	0.05	0.5
SO unstable	$G_8 = 1/(s^2-1)$	-1	j	0	10	0.1	0.05	0.5
	$G_9 = 1/(s(s+1))$	1	1	-	10	0.1	0.05	0.5
Integrating	$G_{10} = 0.1/(s(2s+1))$	0.1	2	-	10	0.1	0.05	0.5
stable	$G_{11} = 1/(s(0.1s+1))$	1	0.1	-	10	0.1	0.05	0.5
Integrating unstable	$G_{12} = 1/(s(s-0.1))$	-10	-10	-	10	0.1	0.05	0.5
	$G_{13} = 100/(s+1)$	100	1	-	10	0.1	0.05	0.5
FO stable	$G_{14} = 1/(1.26s+1)$	1	1.26	-	10	0.1	0.05	0.5
FO unstable	$G_{15} = 100/(s-1)$	-100	-1	-	10	0.1	0.05	0.5
Integrator	$G_{16} = 1/s$	1	10^8	-	10	0.1	0.05	0.5

Next in the test-bench of first order integrating systems with the structure (35), three stable processes are chosen as reported in [32], [34] and [35]. Process G_{10} represents a tank level control with first order actuator or sensor dynamics where input is valve position and process G_{11} represents a simplified automatic controlled dc motor where the input is current and output is the speed. They are given by:

$$G_9(s) = \frac{1}{s(1+s)}, \tag{79}$$

$$G_{10}(s) = \frac{0.1}{s(2s+1)}, \tag{80}$$

$$G_{11}(s) = \frac{1}{s\left(\frac{s}{10}+1\right)}. \tag{81}$$

Next an unstable integrating process is also considered as in [36] and given by:

$$G_{12}(s) = \frac{1}{s(s-0.1)}. \tag{82}$$

Finally, in order to show relatively simpler first order systems having the structure (52), four examples are chosen from [37], the first two (G_{13}, G_{14}) showing stable, the third one (G_{15}) being unstable and the last one (G_{16}) exhibiting integrating open loop dynamics. In particular, within the same first order system template (52), using a very high time constant and DC gain of $K = \tau = 10^8$, closely represent an ideal integrating process. They are represented as:

$$G_{13}(s) = \frac{100}{s+1}, \tag{83}$$

$$G_{14}(s) = \frac{1}{1.26s+1}, \tag{84}$$

$$G_{15}(s) = \frac{100}{s-1}, \tag{85}$$

$$G_{16}(s) = \frac{1}{s}. \tag{86}$$

In our simulations for all the cases, the pole placement parameter and the closed loop damping are chosen as m = 3 and ζ_{cl} = 0.9 respectively as per the guidelines of [6]. Rest of the parameters especially the sampling time for the digital PID controller has been chosen as a fraction of the demanded closed loop time constant until a fairly accurate response is observed (usually kept as T_s/τ_{cl} = 0.5) and shown in Table 1. The upper bound of the desired frequency (ω_{cl}) has been chosen in such way to avoid frequency folding because the sampling theorem may no longer be satisfied [28]. The maximum demanded closed loop frequency (ω_{cl}) should be limited by the choice of sampling time (T_s) in the discrete time implementation of the PID controlled system as $\omega_{\max} > \omega_s/2 = \pi f_s = \pi/T_s = 62.83$ rad/s for $T_s = 0.05$ sec. For the three classes of systems viz. second order, first order integrating and first order with both stable and unstable open-loop dynamics, considering the same template can allow one to model a wide class of processes as shown in Table 1, where open loop unstable systems can be modeled with negative or imaginary damping or time constants with negative DC gains. Using the analytical expressions reported in the previous sections, the PI/PID controller gains can be easily calculated and shown in Table 2 for the 16 test-bench processes.

Table 2: PI/PID controller gains for the test-bench processes for desired specification $m = 3$, $\zeta_{cl} = 0.9$, $\omega_{cl} = 10$

Class of systems	Process model	K_i	K_p	K_d
SO stable	$G_1 = 1/(s^2+1)$	2700	585	45
	$G_2 = 1/(s^2+36)$	2700	550	45
	$G_3 = 1/(s+0.2)^2$	2700	585.96	44.6
	$G_4 = 1/(s+1)^2$	2700	585	43
	$G_5 = 1/((1+0.2s)(1+s))$	540	116.2	7.8
SO unstable	$G_6 = 1/(s-0.2)^2$	2700	585.96	45.4
	$G_7 = 4/(s+4)(s-1)$	675	147.5	10.5
	$G_8 = 1/(s^2-1)$	2700	587	45
Integrating stable	$G_9 = 1/(s(s+1))$	2700	586	44
	$G_{10} = 0.1/(s(2s+1))$	54000	11720	890
	$G_{11} = 1/(s(0.1s+1))$	270	58.6	3.5
Integrating unstable	$G_{12} = 1/(s(s-0.1))$	2700	586	45.1
FO stable	$G_{13} = 100/(s+1)$	1	0.17	-
	$G_{14} = 1/(1.26s+1)$	126	21.68	-
FO unstable	$G_{15} = 100/(s-1)$	1	0.19	-
Only integrator	$G_{16} = 1/s$	100	18	-

5.2. Visualization of PI/PID controller gains as function of given and desired system parameters

It is clear for all the three classes of systems that the PID controller gains depend both on the open loop $\{K, \tau, \zeta_{ol}\}$ and desired closed loop parameters $\{m, \omega_{cl}, \zeta_{cl}\}$. For a fixed non-dominance pole placement parameter $m = 3$ as per the guidelines of [6], the required variation in the three controller gains as a function of damping and frequency of the desired closed loop system is shown in Figure 2, Figure 3, and Figure 4 for the second order (G_6), first order integrating (G_{12}) and first order (G_{13}) processes respectively. In practice, the change in the system DC gain (K) can be easily balanced by linearly decreasing the PID controller gains, and hence its effect is not shown in the figures. However, rest of the parameters $\{\tau, \zeta_{ol}, \omega_{cl}, \zeta_{cl}\}$ have more complex relation on the controller gains and can be shown as 2D maps where the design specifications and process parameters are varied within specified ranges.

The 2D plots of controller gains in Figure 2, Figure 3, and Figure 4 are particularly helpful in getting an idea about which parameters do not affect a particular gain or may have more influence on certain gains. This is evident from the parallel lines along either the *x*-axis or *y*-axis. For the second order system, joint influence of $\{\tau, \omega_{cl}, \zeta_{cl}\}$ on the all three PID controller gains are high as revealed from Figure 2, whereas the effect of open loop damping (ζ_{ol}) has minimal effect on the PID controller gains. This is because the expressions for $\{K_i, K_p\}$ do not contain the term ζ_{ol} and only influence the derivative gain (K_d) as shown in (19). Figure 3 depicts the influence of the PID controller gains as a function of $\{\tau, \omega_{cl}, \zeta_{cl}\}$ for the first order integrating process as obtained from expression (40). It is evident from Figure 3 that the all the three PID controller gains depend on the free parameters $\{\tau, \omega_{cl}, \zeta_{cl}\}$. In particular, higher desired damping and frequency $\{\zeta_{cl}, \omega_{cl}\}$ are likely to increase the three PID controller gains, which can also be verified from the expression in (40). Again, from (59) it is seen for the first order systems the

influence of the two PI controller gains are dependent on the free parameters $\{\tau, \omega_{cl}, \zeta_{cl}\}$ which are shown in Figure 4. However, the integral gain (K_i) in the PI controller for first order system in Figure 4 does not have any effect on the desired closed loop damping (ζ_{cl}), following the expression in (59). However, the proportional gain (K_p) in the PI controller for first order system needs a high value when both the desired closed loop damping and frequency $\{\zeta_{cl}, \omega_{cl}\}$ increase.

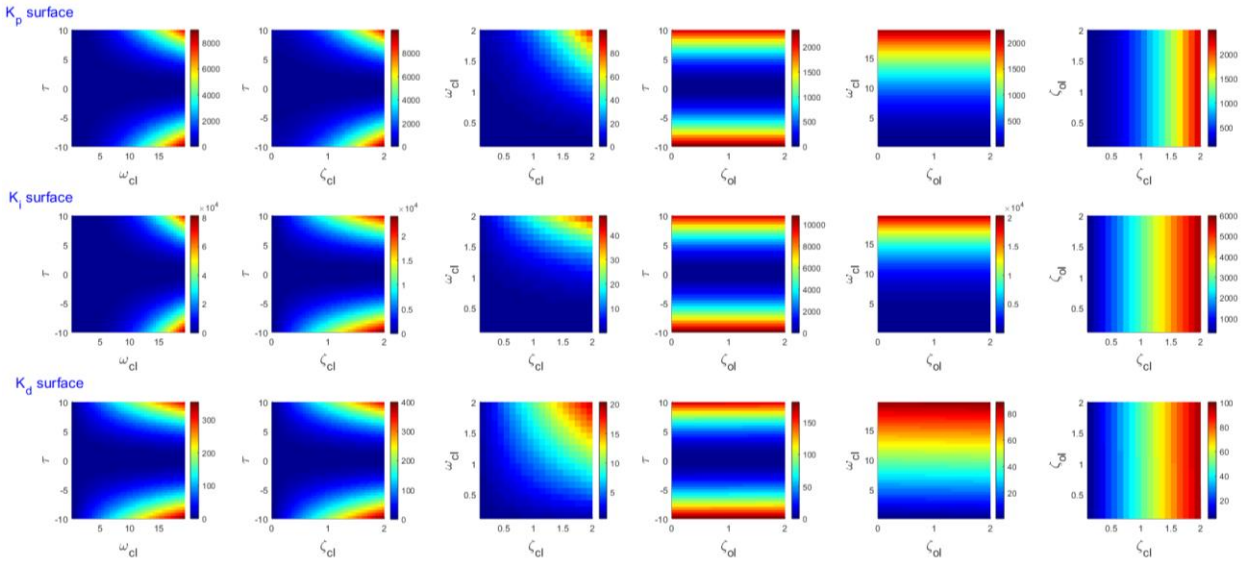

Figure 2: Required variation in the PID controller gains as a function of open loop time constant (τ), desired closed loop damping (ζ_{cl}) and closed loop frequency (ω_{cl}) for second order model with DC gain $K = 25$, $\tau = 5$, $\zeta_{ol} = -1$ (G_6) and desired closed loop parameters $\zeta_{cl} = 0.9$, $\omega_{cl} = 10$.

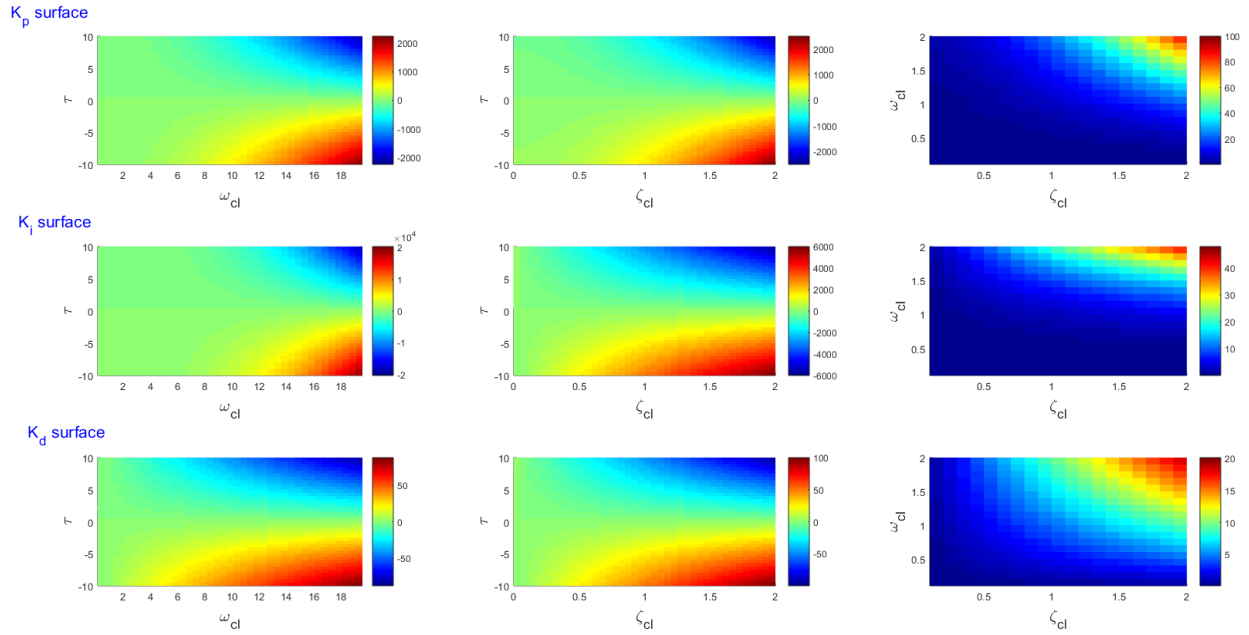

Figure 3: Required variation in the PID controller gains as a function of open loop time constant (τ), desired closed loop damping (ζ_{cl}) and closed loop frequency (ω_{cl}) for first order integrating model with DC gain K = -10, τ = -10 (G_{12}) and desired closed loop parameters $\zeta_{cl} = 0.9$, $\omega_{cl} = 10$.

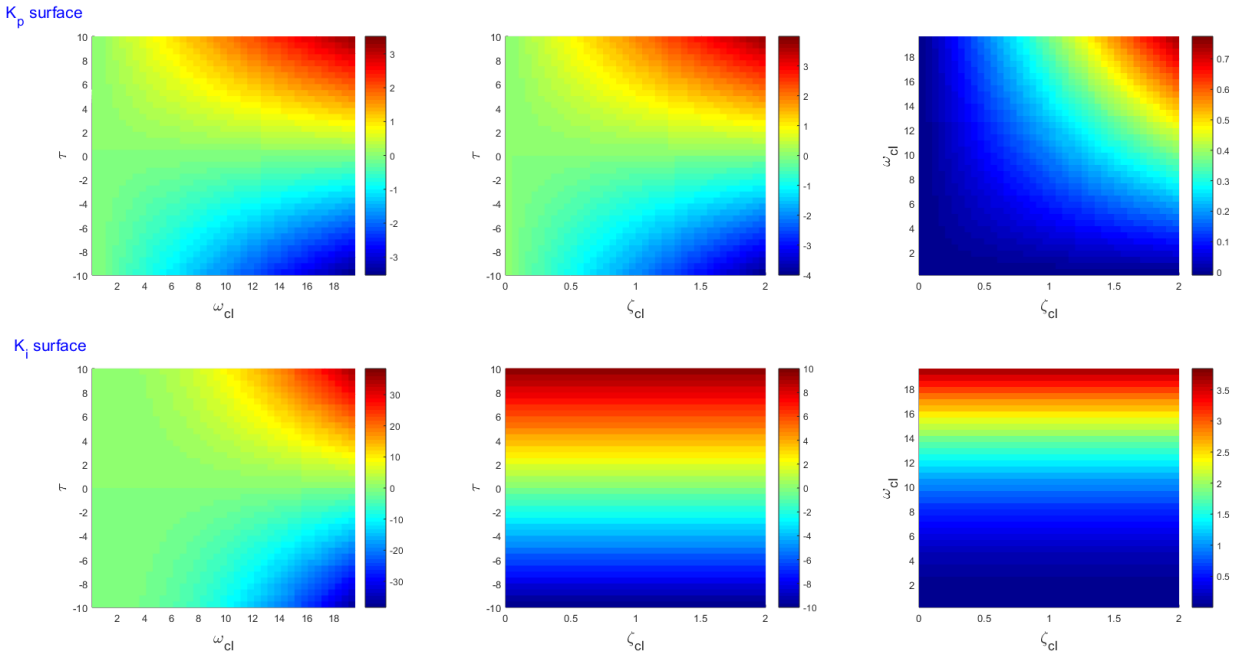

Figure 4: Required variation in the PI controller gains as a function of open loop time constant (τ), desired closed loop damping (ζ_{cl}) and closed loop frequency (ω_{cl}) for first order model with DC gain K = 100, τ = 1 (G_{13}) and desired closed loop parameters $\zeta_{cl} = 0.9$, $\omega_{cl} = 10$.

5.3. Performance comparison between the optimal continuous and discrete time PI/PID controllers

In this section, guaranteed dominant pole placement based PID controller gains in Table 2 are used to compare different performance measures for the test-bench processes between the continuous and discrete time implementations. The Tustin's method or bilinear transform ($s = (2/T_s)\left((1-z^{-1})/(1+z^{-1})\right)$) has been used to obtain the discretized form of the continuous time test-bench processes. To obtain the different performance measures, the unit step input responses for set-point tracking ($CG/(1+CG)$) and the load disturbance rejection task ($G/(1+CG)$) have been shown in the upper panels of Figure 5a (second order), Figure 6a (first order integrating), Figure 7a (first order). This is followed by comparisons of the associated control signals in the bottom panels of Figure 5b (second order), Figure 6b (first order integrating), Figure 7b (first order), for step input tracking ($C/(1+CG)$) and load disturbance rejection task ($1/(1+CG)$) using both continuous and discrete time implementation of the test-bench systems with PI/PID controller gains given in Table 2, where the corresponding desired closed loop specification are given in Table 1. Both the disturbance rejection and tracking performance are found to be almost identical in discrete time with its continuous time version in spite of a relatively large sampling time, compared as a fraction of the desired time constant T_s/τ_{cl} = 0.5 and consequently T_s = 0.05 sec. However, for the control signal associated with set-point tracking, the corresponding transfer function $(C/(1+CG))$ is often improper for the ideal PID controller structure without a derivative filter, having more zeroes than

the number of poles which may not meet the internal stability criteria apart from only the bounded input bounded output (BIBO) stability [38]. In such a situation, it is often not possible to directly simulate a step response control signal from the transfer function $\left(C/(1+CG)\right)$ directly. Here in order to obtain the step response for the control signals associated with tracking, for the second order and first order integrating systems, first we have multiplied a step $(1/s)$ with the transfer function $\left(C/(1+CG)\right)$ which makes the overall transfer function proper, followed by an impulse input excitation. This implementation allows one to easily simulate the equivalent control signals subjected to step input for even an improper transfer function *via* an impulse response of the same transfer function with an additional integrator. The transfer functions for control signal associated with tracking $\left(C/(1+CG)\right)$ for the first order systems and the control signals subjected to a step disturbance input $\left(1/(1+CG)\right)$ for all the three system structures are proper and hence a direct step input response for the control signal can be easily obtained which has been demonstrated in Figure 5b-Figure 7b bottom panels.

The dominant pole placement tuning of PI/PID controller and its fusion with the both continuous and discrete time LQR theory have been shown here to derive the optimal PI/PID controller gains. Here we derive the analytical expressions for the continuous time LQR matrices i.e. weighting matrix and Riccati matrix solution $\{\mathbf{Q},\mathbf{P}\}$ from (15), (20)-(21) for the second order, (42)-(44) for the first order integrating and (62)-(64) for the first order generalized system structures, with a fixed weighting factor $\mathbf{R}$, using the dominant pole placement based PI/PID controller tuning method and CARE (11) as an extension of the works reported in [12], [20], [19], [39]. This is fundamentally different approach where we aim to derive analytical expressions for the LQR weighting matrices and Riccati matrix solution to meet given closed loop performance specifications, compared to the traditional approaches of LQR weight tuning to optimize for certain control performance objectives [40], [22]–[24]. Using the expressions of $\{\mathbf{Q},\mathbf{P}\}$ from (15), (20)-(21) for the second order, (42)-(44) for the first order integrating and (62)-(64) for the first order systems are plugged into the CARE (11) solver to find out the PI/PID controller gains in Table 2 for the test-bench processes in Table 1, while considering the weighting factor as $\mathbf{R}=1$. However, in order to obtain the same discrete PI/PID controller gains from DARE (25) as in continuous time version, here we derive the analytical expressions of the discrete time transformed LQR weighting matrix and discrete Riccati matrix solution $\{\mathbf{Q},\mathbf{P}\}$ as shown in (30)-(34), (48)-(51) and (68)-(70) for the generalized second order (1), first order integrating (35) and first order (52) system templates respectively, while keeping $\mathbf{R}$ fixed and with arbitrary sampling time T_s, which are the main contributions of this paper. Then DARE (25) is also solved using the matrices $\{\mathbf{Q},\mathbf{P}\}$ as in (30)-(34), (48)-(51) and (68)-(70) for second order, first order integrating and first order test-bench processes respectively as reported in Table 1, with the sampling time taken as T_s = 0.05 sec and discrete/continuous time LQR weighting factor $\mathbf{R}=\mathbf{R}=1$ which produce the same PI/PID controller gains as with its continuous time version and shown in Table 2. Thus, it can be observed that the choice of sampling time in discrete LQR has minimal effect to obtain the same PI/PID controller gains as in the continuous time version up to T_s/τ_{cl} = 0.5 and consequently T_s = 0.05 sec for desired τ_{cl} = 0.1 (i.e. $\omega_{cl} = 1/\tau_{cl}$ = 10). This PI/PID controller gains are used next to compare the different performance measures for the test-bench second order, first order integrating, and first order processes given in Table 1, between the continuous and discrete time implementations of the control system. It is evident from Figure 5-Figure 7 that in the discrete PI/PID controller implementation, even with a relatively large sampling time to desired closed-loop time constant ratio i.e. T_s/τ_{cl} = 0.5, the controlled and manipulated variables, in other words, the closed loop system output and the control signals for both the set-point tracking (servo) and load-disturbance rejection (regulatory) tasks, can be maintained as almost identical to their original continuous time versions. Again, it is obvious the unit step responses of the test-bench processes and their control signals for tracking and disturbance rejection task

will also be maintained as identical with finer sampling time $T_s < 0.05\,\text{sec}$, which are not shown here for brevity.

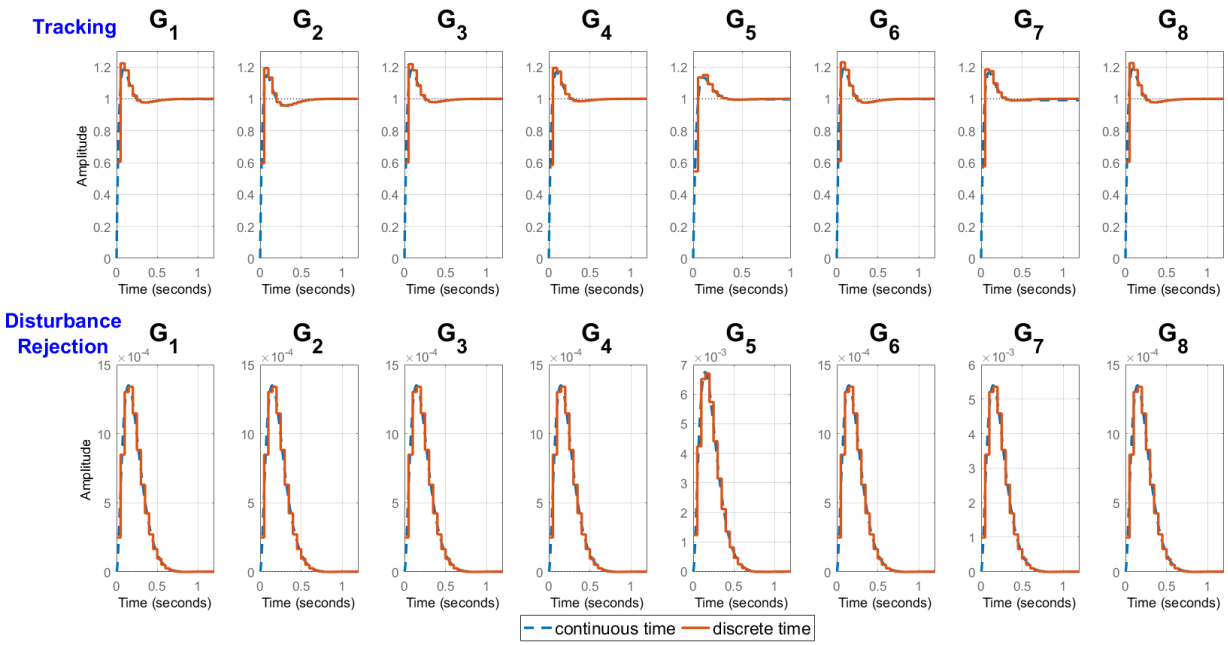

(a)

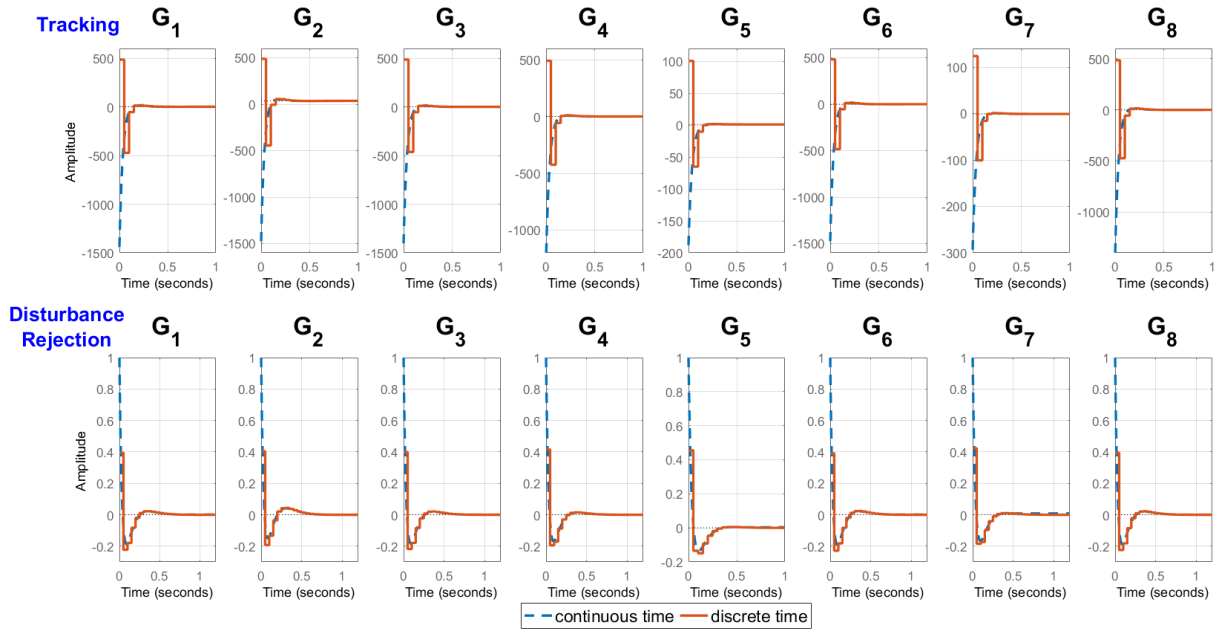

(b)

Figure 5: Unit step response of the continuous and discrete time second order systems (a) step response for tracking and disturbance rejection, (b) associated control signals.

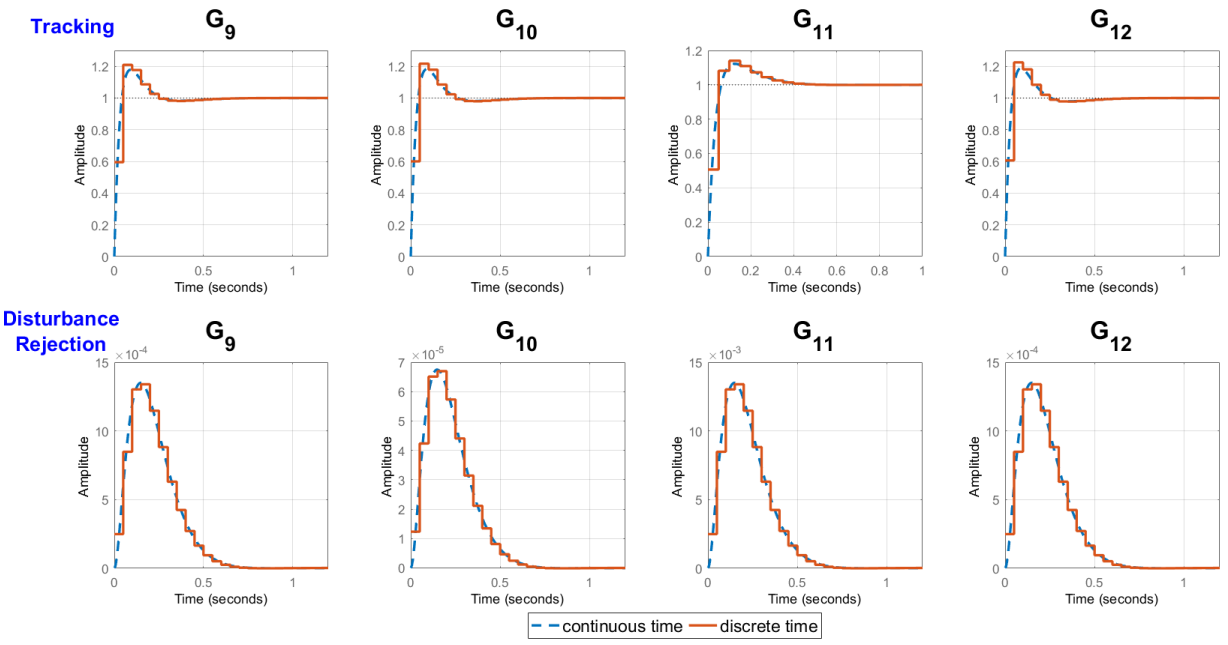

(a)

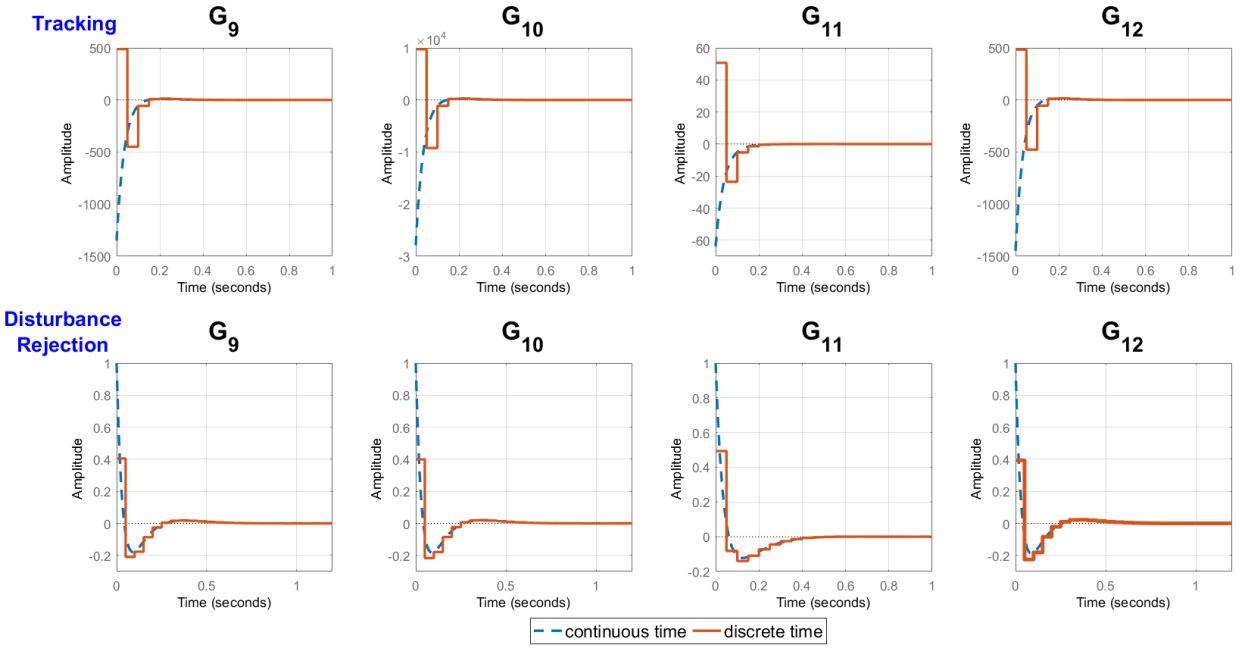

(b)

Figure 6: Unit step response of the continuous and discrete time first order integrating system (a) step response for tracking and disturbance rejection, (b) associated control signals.

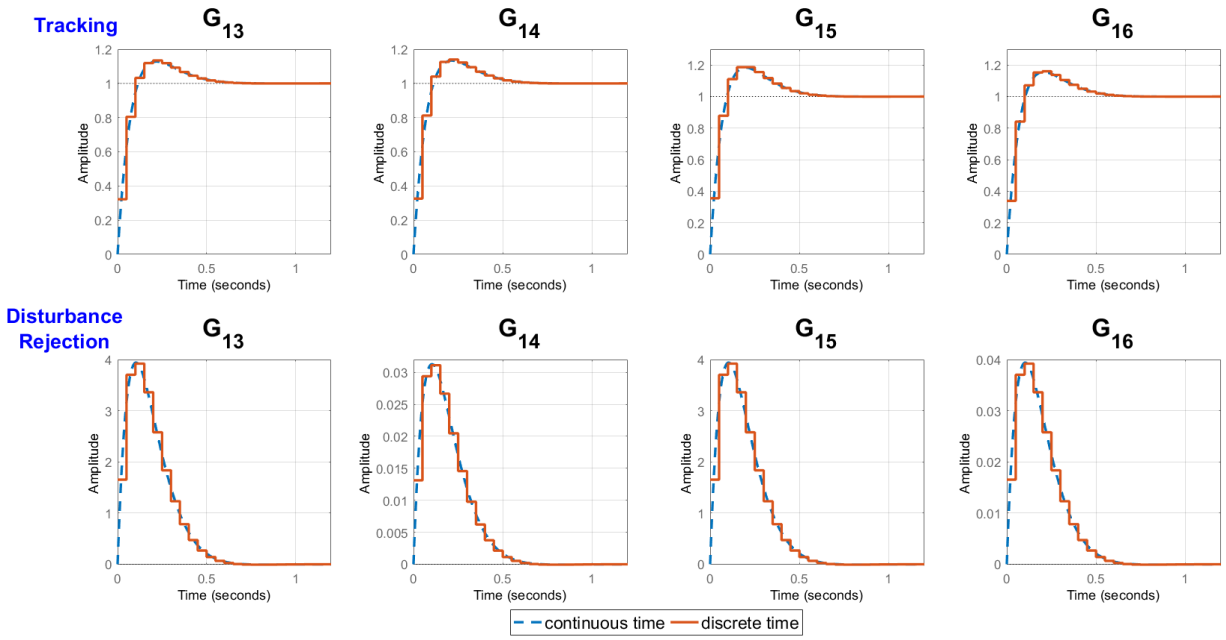

(a)

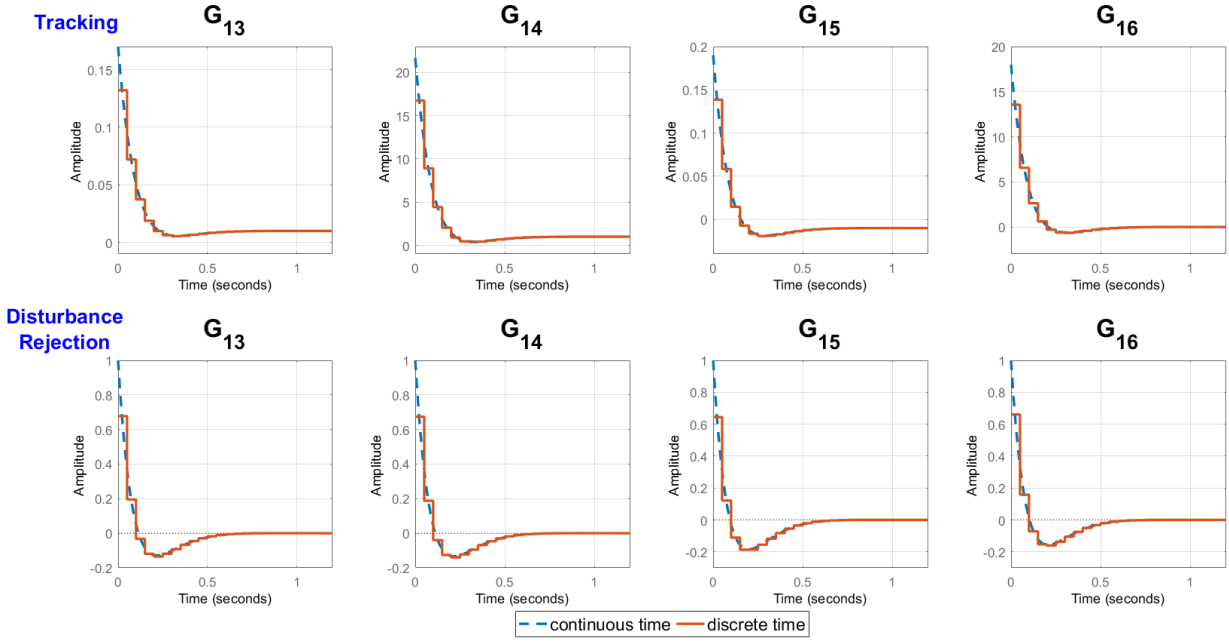

(b)

Figure 7: Unit step response of the continuous and discrete time first order system (a) step response for tracking and disturbance rejection, (b) associated control signals.

Now, the closed loop pole locations and the root locus of the open loop stable/unstable system for the discrete time second order, first order integrating and first order test-bench processes in Table 1 are also shown in Figure 8a, b, c respectively. The root locus of all the test-bench processes have been shown in Figure 8 with a variation in the sampling time between T_s = 0.01-0.05 sec for the first order and first order integrating processes and T_s = 0.01-0.03 sec for the second order processes. It is evident from Figure 8

that the closed loop poles are laying on the root locus branches by changing their position due to the different choice of the sampling time T_s. It is also observed that the closed loop poles are located on the same user demanded damping curve $(\zeta_{cl} = 0.9)$, in the discrete time complex z-plane. Again, the non-dominant and dominant closed loop poles are shifted towards high frequency with increasing T_s. Hence, the proposed methodology guarantees the dominant pole placement using optimal discrete LQR based PI/PID controller which is able to produce the sampling time invariant performances compared to its continuous time implementation, up to a maximum sampling time T_s, bounded by the ratio $T_s/\tau_{cl} = 0.5$.

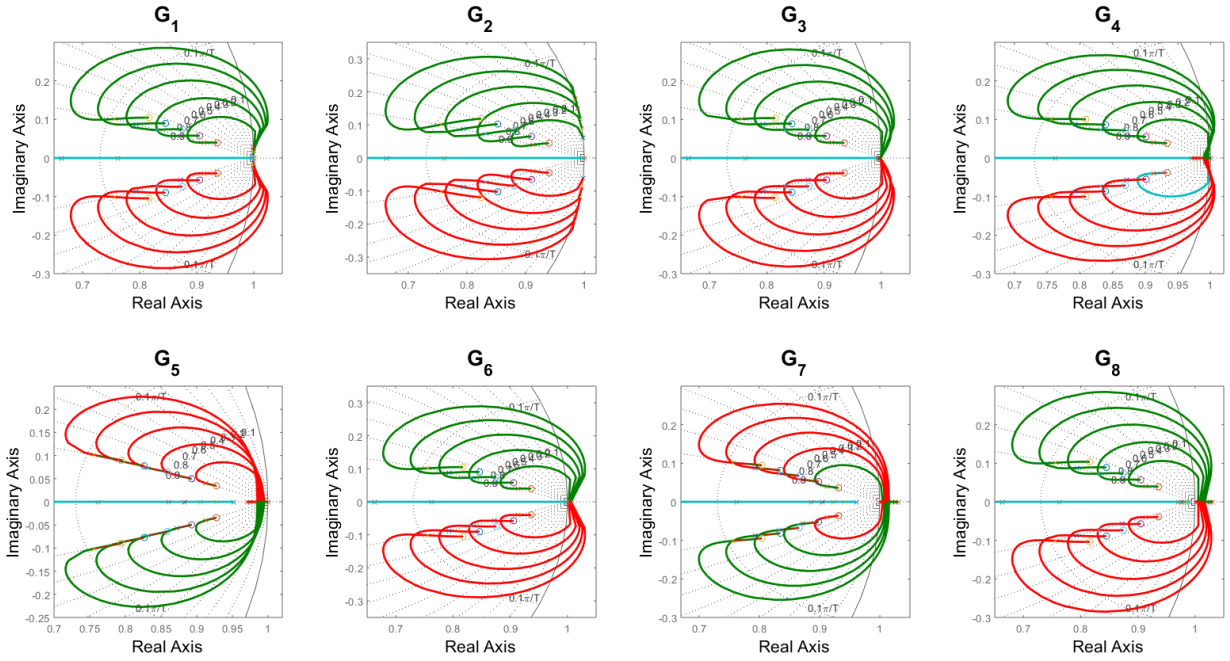

(a)

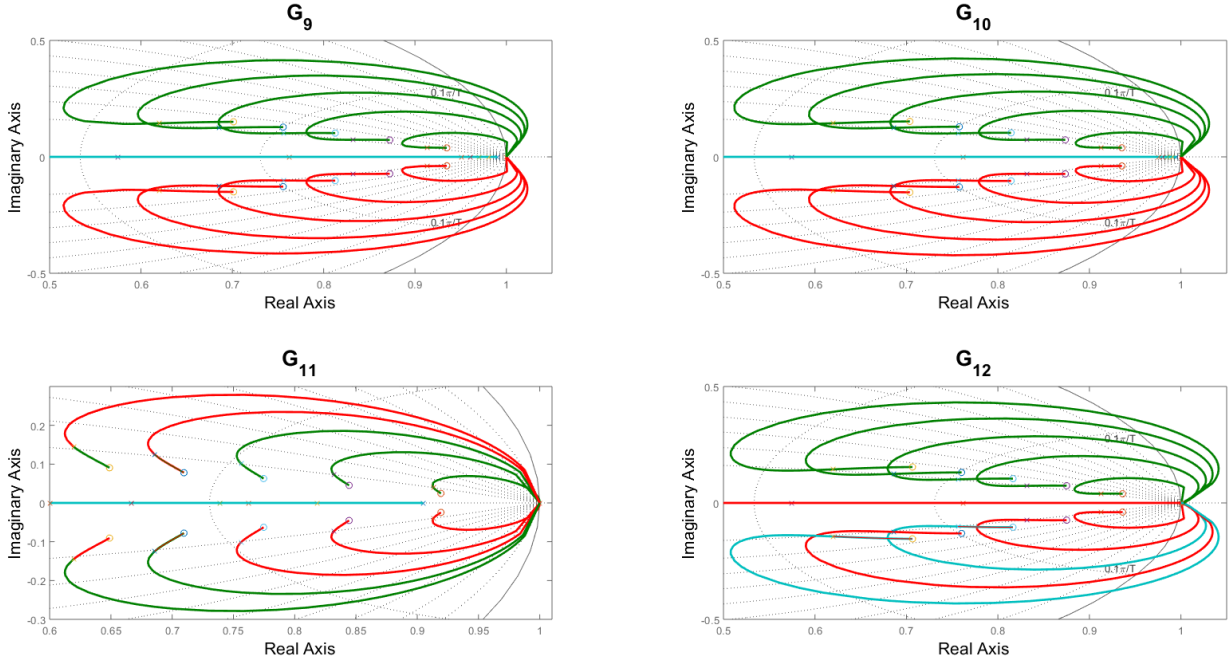

(b)

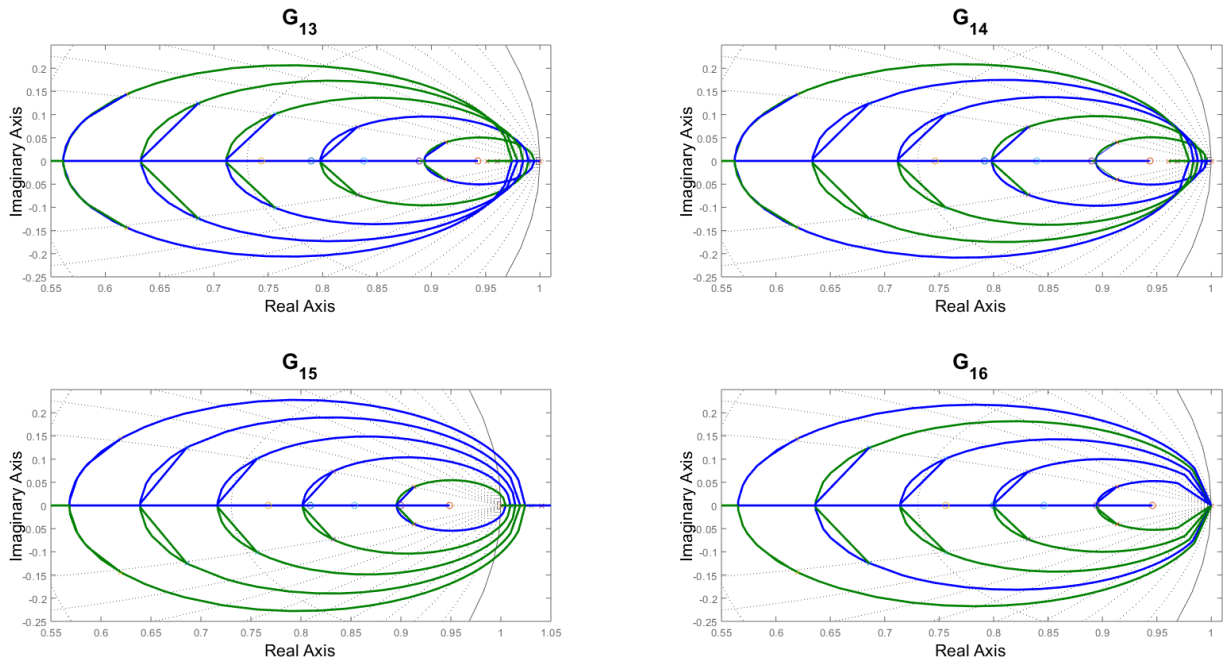

(c)

Figure 8: Root locus (zoomed version) for the test-bench processes (a) second order, (b) first order integrating, (c) first order.

The open and closed loop poles and zeros are also clearly identifiable from the root locus plots. Moreover, it is noticeable that in certain cases the root locus branches goes outside the unit circle for certain ranges of gains for which the system becomes unstable, thus indicating a conditionally stable system. However, the root locus trajectories are stretched more towards the edge of the unit circle and in certain cases a part of the root locus trajectories go outside the unit circle as the sampling time increases. This intuitively confirms our understanding that the performance and stability of a discrete time control system becomes worse with increase in the sampling time.

6. Discussions

In order to achieve an identical time response of a linear system with first order, second order and first order integrating templates by using an optimal controller, the required analytical derivations of the weighting matrices between the continuous and discrete time LQR involving the sampling time (T_s) are the main contributions of this paper. As the aim here is to closely match the discrete and continuous time PI/PID controlled responses in time domain, it is important to check whether the gains obtained in the continuous time optimal pole placement problem can still be used in the discrete time version, without the loss of optimality due to discretization with arbitrarily large sampling time. To achieve this, this paper proposes to modify only the diagonal elements of the discrete time LQR weighting matrix $\mathbf{Q}$ using equations (33), (51) and (69) for second order, first order integrating and first order template respectively, while keeping the weighting factor fixed ($\mathbf{R} = \mathbf{R} = 1$) for both the continuous and discrete time. Use of the LQR optimal control theory, in respective continuous and discrete time PI/PID controllers ensures the state vs. control effort optimality, subjected to a suitable choice of sampling time. Our methodology shows even if the sampling time is chosen arbitrarily large (although being bounded by the desired closed loop time constant τ_{cl}), the discrete time LQR weighting matrix can be analytically derived in such a way

that the PI/PID controller gains and the corresponding set-point tracking and disturbance rejection performances are close enough with its continuous time version and hence can readily be used in a digital implementation of an industrial control system set-up. To demonstrate the utility of the proposed methodology for maintaining identical time response in both the continuous and discrete time, depending on the desired closed loop performance, there is a unique LQR weighting matrix ($\mathbf{Q}$) for CARE solver. But to obtain the same time domain performance, the discrete LQR weighting matrix ($\mathbf{Q}$) for DARE solver needs to be updated accordingly using the respective expressions, depending on the sampling time and the type of system under control.

It is well-known that the closed loop system become unstable when T_s is increasing to an arbitrarily large value [22]. Depending on the relative stability of a system under control which can often be assessed using the ratio (T_s/τ), one can choose the sampling time T_s. For example, a first order (52) or first order integrating (35) system, with a pole at $s=-1/\tau$ will have less relative stability for a large time constant (say $\tau=1, s=-1$) compared to a small time constant (say $\tau=0.1, s=-10$), because the pole of the latter case lie far away from the imaginary axis in the complex *s*-plane and less prone to instability. Whereas for negative time constants as seen in unstable systems, the observation is opposite i.e. a large negative time constant (say $\tau=-1, s=1$) has better relative stability compared to a small negative time constant (say $\tau=-0.1, s=10$) as the latter case has unstable pole far away from the imaginary axis and in the unstable positive half region of the complex *s*-plane, which are much harder cases to attract by the PI/PID controller zeros so that the stabilized closed loop poles lie only in the negative half of complex *s*-plane. Therefore, for a system with higher relative stability (T_s/τ) a larger T_s can be applied [41]. According to the increasing relative stability criteria, therefore the four processes can be ranked as: $\tau=\{-0.1,-1,+1,+0.1\}$, since their relative stability measure increases as: $(T_s/\tau)=\{-0.1,-0.01,0.01,0.1\}$, for a fixed sampling time $T_s=0.01$ sec. A similar criterion can also be derived for the second order system where along with the open loop time constant, the damping also plays an important role in judging the relative stability of the system. However, in this paper we choose the maximum allowable sampling time based on the desired closed loop time constant (T_s/τ_{cl}) which has been demonstrated for various types of test-bench processes in Table 1.

Although we proposed here a novel way for discrete LQR based digital PI/PID controller design with a discretization invariant transformation between continuous and discrete times, there are also a few limitations of the presented approach, as outlined below:

- The design is based on fixing the weighting factor $\mathbf{R}=\mathbf{R}$ first between the continuous and discrete time versions and then deriving the transformation between the respective $\{\mathbf{Q},\mathbf{Q}\}$ matrices, unlike the simultaneous LQR weighting matrix and weighting factor $\{\mathbf{Q},\mathbf{R}\}$ tuning as reported in [40], [22]–[24]. This is a widely used analytical approach for LQR based PID controller design for SISO systems [12], [20], [19], [39], as the $\mathbf{R}=\mathbf{R}$ matrix are mere constants which greatly helps in the analytical derivation rather than including it in the expressions for the PI/PID controller gains. However, for MIMO systems such a design can be extended with different choice of both the $\{\mathbf{Q},\mathbf{R}\}$ matrices, in a future research.

- The derived expressions of $\{\mathbf{Q},\mathbf{Q}\}$ matrices depend on the choice of $\{\mathbf{R},\mathbf{R}\}$ which are considered to be the same. If $\{\mathbf{R},\mathbf{R}\}$ are modified, the associated $\{\mathbf{Q},\mathbf{Q}\}$ matrices also change, thus affecting the closed loop performance of the PID controlled system [22], [24]. However, this paper does not

address simultaneous choice of both the LQR design matrices but considers that the weighting factors $\{\mathbf{R},\mathbf{R}\}$ to be fixed and then derives the transformation of the associated weighting matrices $\{\mathbf{Q},\mathbf{Q}\}$.

- The present design incorporates the choice of sampling time T_s in the selection of $\mathbf{Q}$ matrix in the discrete time LQR. However, a large value of sampling time will make the control system's response unusable, for any real-world application. Often the choice of T_s depends on the instrumentation and is considered as a fixed fractional value of the dominant time constant of the system i.e. (T_s/τ_{cl}). However, this paper does not directly address the issue of optimal choice of the sampling time to discretize the continuous time PID controller but derives a criterion to obtain similar closed loop performance, in spite of variation in the sampling time. For simulation studies it considers an upper bound on the $T_s/\tau_{cl}=0.5$ for which both the servo/regulatory responses on the controlled and manipulated variables are found to be close enough.

- Our design in the present context neglects a dominant zero dynamics and significantly large time delay in the open loop system which cannot be accurately reduced to one of the three templates considered here viz. second order, first order integrating and first order template, in spite of their wide applicability to capture many real industrial processes, including even higher order process dynamics with negligibly small delays and weak lead effect. The main obstacle to extend the same dominant pole placement approach for time delay systems is that a large delay is manifested as infinite number of poles/zeros and deriving the dominance with infinite number of poles becomes infeasible using the present approach as previously discussed in [6] which can be explored in a future research. Also, because of the inherent feature of placing only the dominant poles in the desired closed loop system, the effect of more complex behaviors like significant zero dynamics (with minimum or non-minimum phase) and delays on top of open loop unstable and marginally stable poles can be pursued as a scope future research.

- The design assumes perfect knowledge of the system models, although in a more realistic case, these models can be uncertain either being norm bounded or with varying parameters within certain intervals. Such robust control designs are usually not considered in either dominant pole placement or LQR based designs and are left as scope for further research.

Moreover, it is important to note that the aim of this paper is designing a dominant pole-placement based PI/PID controller that yields specified closed loop performance measures. Next, we find out an inverse optimality condition for this particular pole-placement problem and derive the weighting matrices and Riccati solution in terms of the open-loop process and desired closed-loop system parameters similar to [12], [20]. Indeed, the forward PID control pole placement problem does not include any direct optimal control principle but it is possible to find out an inverse optimal control equivalence for this pole placement problem where the optimal state feedback gains, obtained through the solution of the Riccati equation are considered as the PID controller gains [12], [20]. Since the pole placement problem is designed in continuous time, the corresponding inverse optimality condition takes the continuous time form as well. However, up on discretizing the controller with arbitrary sampling time, the equivalent discrete time inverse optimality conditions may not hold which also indicate degradation of the closed loop performance. For the discrete time equivalent inverse optimal control problem, therefore the discrete LQR weighting matrices need to be adjusted accordingly, so that the specified performances in terms of the dominant closed loop pole locations are preserved, even after discretization with arbitrary sampling time. Therefore, the results need to be interpreted carefully as the PID controller design problem is not motivated to be optimal in traditional sense, since the underlying control principle is dominant-pole placement. The corresponding inverse optimal control problems have been analyzed then i.e. the

equivalent continuous and discrete time LQR versions of the pole-placement problem are dealt with in the form of discretization with arbitrary sampling time and still maintaining similar closed-loop servo-regulatory responses.

7. Conclusion

This paper proposes a novel methodology for the design of discretization invariant digital PI/PID controllers to handle a family of second order, first order integrating and first order systems, using the concepts of guaranteed dominant pole placement. We also derive the corresponding inverse optimality conditions for the dominant pole placement based PI/PID control problem in terms of continuous and discrete time LQR. The main contribution of the paper is to derive a novel transformation of the discrete time LQR weighting matrix ($\mathbf{Q}$) to obtain the same PI/PID controller gains in discrete time, irrespective of the choice of sampling time to match the performance of the continuous time LQR based PID control loop. Simulation examples are shown on test-bench processes with different sampling times to investigate the discrete time closed-loop pole locations, meeting the specified continuous time closed loop performances. The advantage of the proposed method is that the same PI/PID controller designed in continuous time can readily be implemented digitally using the proposed transformation, without sacrificing the quality of the time domain control performances like tracking, disturbance rejection and controller effort. Future scope of research may include extending the methodology for systems with large process delay and dominant zero dynamics.

Acknowledgement

KH acknowledges the support from the University Grants Commission (UGC), Govt. of India under its Basic Scientific Research (BSR) scheme. SD was partially supported by the ESIF ERDF Cornwall New Energy project.

References

[1] K. J. Åström and T. Hägglund, *PID controllers: theory, design, and tuning*, vol. 10. 1995.

[2] P. Cominos and N. Munro, "PID controllers: recent tuning methods and design to specification," *IEE Proceedings-Control Theory and Applications*, 2002, vol. 149, no. 1, pp. 46–53.

[3] K. Ogata, *Modern Control Engineering*. Prentice Hall PTR, 2001.

[4] B. D. Anderson and J. B. Moore, *Optimal control: linear quadratic methods*. Courier Corporation, 2007.

[5] P. Dorato and A. H. Levis, "Optimal linear regulators: the discrete-time case," *IEEE Transactions on Automatic Control*, vol. 16, no. 6, pp. 613–620, 1971.

[6] Q.-G. Wang, Z. Zhang, K. J. Astrom, and L. S. Chek, "Guaranteed dominant pole placement with PID controllers," *Journal of Process Control*, vol. 19, no. 2, pp. 349–352, 2009.

[7] W. Tang, Q.-G. Wang, Z. Ye, and Z. Zhang, "PID tuning for dominant poles and phase margin," *Asian Journal of Control*, vol. 9, no. 4, pp. 466–469, 2007.

[8] H. I. Kang, "Design of dominant pole region assignment with PID controllers," *2010 International Conference on Intelligent Computation Technology and Automation (ICICTA)*, 2010, vol. 2, pp. 19–22.

[9] A. Madady and H.-R. Reza-Alikhani, "First-order controllers design employing dominant pole placement," *2011 19th Mediterranean Conference on Control & Automation (MED)*, 2011, pp. 1498–1503.

[10] L. Yinya, S. Andong, and Q. Quoqing, "Further results on guaranteed dominant pole placement with PID controllers," *2011 30th Chinese Control Conference (CCC)*, 2011, pp. 3756–3760.

[11] I. G. Velásquez, J. I. Yuz, and M. E. Salgado, "Optimal control synthesis with prescribed closed loop poles," *2011 19th Mediterranean Conference on Control & Automation (MED)*, 2011, pp. 108–113.
[12] S. Das, K. Halder, I. Pan, S. Ghosh, and A. Gupta, "Inverse optimal control formulation for guaranteed dominant pole placement with PI/PID controllers," *2012 International Conference on Computer Communication and Informatics (ICCCI)*, 2012, pp. 1–6.
[13] T. Fujii, "A new approach to the LQ design from the viewpoint of the inverse regulator problem," *IEEE Transactions on Automatic Control*, vol. 32, no. 11, pp. 995–1004, 1987.
[14] T. Fujii and M. Narazaki, "A complete solution to the inverse problem of optimal control," *1982 21st IEEE Conference on Decision and Control*, 1982, no. 21, pp. 289–294.
[15] P. J. Moylan and B. Anderson, "Nonlinear regulator theory and an inverse optimal control problem," *IEEE Transactions on Automatic Control*, vol. 18, no. 5, pp. 460–465, 1973.
[16] K. Sugimoto, "Partial pole placement by LQ regulators: An inverse problem approach," *IEEE Transactions on Automatic Control*, vol. 43, no. 5, pp. 706–708, 1998.
[17] Y. Choi and W. K. Chung, "Performance limitation and autotuning of inverse optimal PID controller for lagrangian systems," *Journal of Dynamic Systems, Measurement, and Control*, vol. 127, no. 2, pp. 240–249, 2005.
[18] T. Fujinaka and T. Katayama, "Discrete-time optimal regulator with closed-loop poles in a prescribed region," *International Journal of Control*, vol. 47, no. 5, pp. 1307–1321, 1988.
[19] J.-B. He, Q.-G. Wang, and T.-H. Lee, "PI/PID controller tuning via LQR approach," *Chemical Engineering Science*, vol. 55, no. 13, pp. 2429–2439, 2000.
[20] S. Saha, S. Das, S. Das, and A. Gupta, "A conformal mapping based fractional order approach for sub-optimal tuning of PID controllers with guaranteed dominant pole placement," *Communications in Nonlinear Science and Numerical Simulation*, vol. 17, no. 9, pp. 3628–3642, 2012.
[21] M. Saif, "Optimal linear regulator pole-placement by weight selection," *International Journal of Control*, vol. 50, no. 1, pp. 399–414, 1989.
[22] S. Das, I. Pan, K. Halder, S. Das, and A. Gupta, "LQR based improved discrete PID controller design via optimum selection of weighting matrices using fractional order integral performance index," *Applied Mathematical Modelling*, vol. 37, no. 6, pp. 4253–4268, 2013.
[23] S. Das, I. Pan, and S. Das, "Multi-objective LQR with optimum weight selection to design FOPID controllers for delayed fractional order processes," *ISA Transactions*, vol. 58, pp. 35–49, 2015.
[24] S. Das and K. Halder, "Missile attitude control via a hybrid LQG-LTR-LQI control scheme with optimum weight selection," *2014 First International Conference on Automation, Control, Energy and Systems (ACES)*, 2014, pp. 1–6.
[25] T. H. Abdelaziz, "Pole placement for single-input linear system by proportional-derivative state feedback," *Journal of Dynamic Systems, Measurement, and Control*, vol. 137, no. 4, p. 041015, 2015.
[26] T. H. Abdelaziz, "Stabilization of single-input LTI systems by proportional-derivative feedback," *Asian Journal of Control*, vol. 17, no. 6, pp. 2165–2174, 2015.
[27] T. H. Abdelaziz, "Stabilization of linear time-varying systems using proportional-derivative state feedback," *Transactions of the Institute of Measurement and Control*, p. 0142331217697787, 2017.
[28] K. Ogata, *Discrete-time control systems*, vol. 2. Prentice Hall Englewood Cliffs, NJ, 1995.
[29] G. F. Franklin, J. D. Powell, and M. L. Workman, *Digital control of dynamic systems*, vol. 3. Addison-wesley Menlo Park, 1998.
[30] V. G. Rao and D. S. Bernstein, "Naive control of the double integrator," *IEEE Control Systems*, vol. 21, no. 5, pp. 86–97, 2001.
[31] K. J. Åström and T. Hägglund, "Benchmark systems for PID control," *IFAC Proceedings Volumes*, vol. 33, no. 4, pp. 165–166, 2000.
[32] B. Kristiansson and B. Lennartson, "Robust tuning of PI and PID controllers: using derivative action despite sensor noise," *IEEE Control Systems*, vol. 26, no. 1, pp. 55–69, 2006.

[33] K. J. Åström, H. Panagopoulos, and T. Hägglund, "Design of PI controllers based on non-convex optimization," *Automatica*, vol. 34, no. 5, pp. 585–601, 1998.
[34] A. Isaksson and S. Graebe, "Derivative filter is an integral part of PID design," *IEE Proceedings-Control Theory and Applications*, vol. 149, no. 1, pp. 41–45, 2002.
[35] O. Yaniv and M. Nagurka, "Robust PI controller design satisfying sensitivity and uncertainty specifications," *IEEE Transactions on Automatic Control*, vol. 48, no. 11, pp. 2069–2072, 2003.
[36] K. Halder, S. Das, S. Dasgupta, S. Banerjee, and A. Gupta, "Controller design for Networked Control Systems—An approach based on L2 induced norm," *Nonlinear Analysis: Hybrid Systems*, vol. 19, pp. 134–145, 2016.
[37] K. J. Åström and T. Hägglund, *Advanced PID control*. ISA-The Instrumentation, Systems and Automation Society, 2006.
[38] J. C. Doyle, B. A. Francis, and A. R. Tannenbaum, *Feedback control theory*. Courier Corporation, 2013.
[39] S. Srivastava, A. Misra, S. Thakur, and V. Pandit, "An optimal PID controller via LQR for standard second order plus time delay systems," *ISA Transactions*, vol. 60, pp. 244–253, 2016.
[40] I. Pan and S. Das, "Design of hybrid regrouping PSO-GA based sub-optimal networked control system with random packet losses," *Memetic Computing*, vol. 5, no. 2, pp. 141–153, 2013.
[41] I. Pan, A. Mukherjee, S. Das, and A. Gupta, "Simulation studies on multiple control loops over a bandwidth limited shared communication network with packet dropouts," *2011 IEEE Students' Technology Symposium (TechSym)*, 2011, pp. 113–118.